DD-R-23(EN)

DANSK DEKOMMISSIONERING

Dismantling the internal parts of research reactor DR 3

A catalogue of radiation fields

Per Hedemann Jensen and Jens Søgaard-Hansen

Danish Decommissioning, Roskilde
September 2010

DD-R-23(EN)

Dismantling the internal parts of research reactor DR 3

A catalogue of radiation fields

Per Hedemann Jensen and Jens Søgaard-Hansen

Danish Decommissioning, Roskilde
September 2010

Author: Per Hedemann Jensen and Jens Søgaard-Hansen

Title: Dismantling the internal parts of research reactor DR 3 – A catalogue of radiation fields

Department: Section of Radiation and Nuclear Safety

DD-R-23(EN)
September 2010

Abstract. The internal parts of reactor DR 3 - the top shield ring, the reactor tank, the graphite reflector and the inner and outer steel tanks - contain about 1 TBq of ^{60}Co at the beginning of 2012. The dismantling of these components requires a detailed planning in order to reduce the exposure of the involved dismantling staff to be as low as reasonable achievable. Radiation fields from the internal components have been calculated with the Monte Carlo code MCNP5. The order of dismantling the internal parts of DR 3 is dictated by the construction of the reactor; therefore, the following sequence of dismantling is more or less fixed: (1) top shield plug, (2) top shield ring, (3) reactor tank, (4) graphite reflector and (5) steel tanks with a lead shield between the tanks. The Monte Carlo calculations of the radiation fields are based on measured and calculated activity concentrations in the different construction parts. The uncertainty of these estimates is considerable and determines the major uncertainty on the calculated radiation fields around the construction parts. The report contains the results of the MCNP5-calculations of the radiation fields that have been used in the planning of an optimal dismantling of the internal parts of reactor DR 3.

ISBN 978-87-7666-034-5
ISBN 978-87-7666-035-2 (Internet)

Group's own reg. no.:
Radiation and Nuclear Safety/DR 3

Pages: 43
Figures: 40
Tables: 21
References: 7

Danish Decommissioning
Post Box 320
4000 Roskilde

Tel.: + 45 4677 4300
Fax: + 45 4677 4302
E-mail: dd@dekom.dk
Web: www.dekom.dk

Contents

1 Introduction

The decommissioning of the research reactor DR 3 is a challenging task due to high γ-radiation levels from the neutron-activated inner constructions parts of the reactor. The dismantling of these components requires a detailed planning in order to reduce the exposure of the involved dismantling staff to be as low as reasonable achievable. The spatial distribution of the γ-radiation fields together with estimated working hours in different radiation fields will determine the exposure of workers involved in decommissioning the inner construction parts of the reactor.

The γ-radiation fields should be assessed before the shielding (top shield plug) of the inner components is removed. The activity concentrations in the different construction parts of the reactor is based upon measured and calculated activity concentrations. There is a considerable uncertainty (50 - 200%) on the characterization of the activity distribution in the different reactor components. As the radiation levels are proportional to the activity content in the different components, estimated radiation levels will at least include this uncertainty, which should be taken into consideration when planning the dismantling of the inner construction parts.

The γ-radiation fields from the activated inner construction parts have been calculated with the Monte Carlo code MCNP5. The calculations are based on measured and calculated activity concentrations in the different construction parts of the reactor as described in the references [1] - [6]. The objective of this report is to present the calculated γ-radiation fields around the inner construction parts. The results have been applied to estimate the individual and collective doses from different dismantling scenarios.

2 Activity distribution in DR 3

The inner construction parts have a relatively high content of activity - mainly ^{60}Co - due to neutron activation during 40 years of operation. The major components include (exclusive the top shield plug):

- top shield ring (TSR)
- aluminium reactor tank (RAT)
    - upper cylinder section
    - middle cylinder section
    - lower cylinder section
    - horizontal experimental tubes
    - bottom cylinder
    - grid plate
    - bottom plate
- graphite reflector
- inner steel tank
    - top flange
    - upper part
    - thick section
    - lower part
    - bottom plate
- outer steel tank

The estimated activity distribution of ^{60}Co in the inner parts of DR 3 at the beginning of 2012 is shown in Table 1.

Table 1. Distribution of ^{60}Co-activity in the internal components of reactor DR 3.

Construction part	R_o	R_i	H_t	H_b	V	ρ	m	C	Q	Q_{rel}	Cell No.	Q_{part}
	[cm]	[cm]	[cm]	[cm]	[cm^3]	[g/cm^3]	[g]	[Bq/g]	[Bq]	[%]		[Bq]
Reactor tank, upper cylinder section	101.60	100.33	378.18	323.45	4.41E+04	2.70	1.19E+05	0.00E+00	0.00E+00	0	1	
Reactor tank, middle cylinder section	101.60	98.43	323.45	255.50	1.35E+05	2.70	3.65E+05	2.39E+04	8.73E+09	0.73	2	
Reactor tank, lower cylinder section	101.60	100.33	255.50	98.99	1.26E+05	2.70	3.40E+05	7.73E+04	2.63E+10	2.20	3	
Reactor tank, tank bottom, cylinder	101.60	100.02	98.99	73.99	2.50E+04	2.70	6.75E+04	5.00E+04	3.38E+09	0.28	4	6.57E+10
Reactor tank, tank bottom, plate	101.60	0.00	73.99	72.40	5.16E+04	2.70	1.39E+05	5.00E+04	6.96E+09	0.58	5	
Grid plate	55.25	0.00	77.25	73.99	3.13E+04	2.70	8.43E+04	7.73E+04	6.52E+09	0.55	6	
Experimental tubes	100.33	52.50	119.88	116.99	6.64E+04	2.70	1.79E+05	7.73E+04	1.38E+10	1.16	7	
Top ring, upper part, steel, top	137.80	101.60	378.18	376.28	5.17E+04	7.86	4.07E+05	0.00E+00	0.00E+00	0.00	8	
Top ring, upper part, steel cylinder, outer	137.80	136.53	376.28	321.99	5.94E+04	7.86	4.67E+05	1.35E+02	6.31E+07	5.273E-03	9	
Top ring, upper part, steel cylinder, inner	102.87	101.60	376.28	321.99	4.43E+04	7.86	3.48E+05	2.70E+03	9.40E+08	7.86E-02	10	
Top ring, upper part, shot concrete	136.53	102.87	376.28	321.99	1.37E+06	5.69	7.82E+06	9.80E+00	7.66E+07	6.41E-03	11	
Top ring, lower part, steel cylinder, outer	134.60	133.33	321.99	263.25	6.28E+04	7.86	4.94E+05	4.43E+04	2.19E+10	1.83	12	
Top ring, lower part, steel cylinder, inner	102.87	101.60	321.99	263.25	4.79E+04	7.86	3.77E+05	8.85E+05	3.33E+11	27.87	13	1.06E+12
Top ring, lower part, shot concrete	133.33	102.87	321.99	276.79	1.02E+06	5.69	5.81E+06	8.96E+02	5.21E+09	0.44	14	
Top ring, lower part, steel plates	133.33	102.87	276.79	273.61	7.19E+04	7.86	5.65E+05	4.55E+03	2.57E+09	0.21	15	
Top ring, lower part, lead	133.33	102.87	273.61	263.45	2.30E+05	11.34	2.60E+06	1.18E+01	3.07E+07	0.00	16	
Top ring, lower part, cadmium	133.33	102.87	263.45	263.25	4.52E+03	8.64	3.91E+04	0.00E+00	0.00E+00	0.00	17	
Top ring, lower part, steel plate bottom	134.60	101.60	263.25	261.98	3.11E+04	7.86	2.44E+05	2.83E+06	6.92E+11	57.85	18	
Graphite, 1st radial layer from top	137.80	101.60	261.98	237.72	6.61E+05	2.20	1.45E+06	3.37E+03	4.90E+09	0.41	19	
Graphite, 2nd radial layer from top	137.80	101.60	237.72	219.94	4.84E+05	2.20	1.06E+06	3.37E+03	3.59E+09	0.30	20	
Graphite, 3rd radial layer from top	137.80	101.60	219.94	202.16	4.84E+05	2.20	1.06E+06	3.37E+03	3.59E+09	0.30	21	
Graphite, 4th radial layer from top	137.80	101.60	202.16	184.38	4.84E+05	2.20	1.06E+06	3.37E+03	3.59E+09	0.30	22	
Graphite, 5th radial layer from top	137.80	101.60	184.38	166.60	4.84E+05	2.20	1.06E+06	3.37E+03	3.59E+09	0.30	23	
Graphite, 6th radial layer from top	137.80	101.60	166.60	148.82	4.84E+05	2.20	1.06E+06	3.37E+03	3.59E+09	0.30	24	
Graphite, 7th radial layer from top	137.80	101.60	148.82	131.04	4.84E+05	2.20	1.06E+06	3.37E+03	3.59E+09	0.30	25	
Graphite, 8th radial layer from top	137.80	101.60	131.04	113.26	4.84E+05	2.20	1.06E+06	3.37E+03	3.59E+09	0.30	26	6.00E+10
Graphite, 9th radial layer from top	137.80	101.60	113.26	95.48	4.84E+05	2.20	1.06E+06	3.37E+03	3.59E+09	0.30	27	
Graphite, 10th radial layer from top	137.80	101.60	95.48	77.70	4.84E+05	2.20	1.06E+06	3.37E+03	3.59E+09	0.30	28	
Graphite, 11th radial layer from top	137.80	101.60	77.70	59.92	4.84E+05	2.20	1.06E+06	3.37E+03	3.59E+09	0.30	29	
Graphite, bottom layer, 1st layer from top	137.80	0.00	59.92	49.07	6.47E+05	2.20	1.42E+06	3.37E+03	4.80E+09	0.40	30	
Graphite, bottom layer, 2nd layer from top	137.80	0.00	49.07	38.22	6.47E+05	2.20	1.42E+06	3.37E+03	4.80E+09	0.40	31	
Graphite, bottom layer, 3rd layer from top	137.80	0.00	38.22	27.37	6.47E+05	2.20	1.42E+06	3.37E+03	4.80E+09	0.40	32	
Graphite, bottom layer, 4th layer from top	137.80	0.00	27.37	16.52	6.47E+05	2.20	1.42E+06	3.37E+03	4.80E+09	0.40	33	
Inner steel tank, top flange	147.95	140.35	378.18	368.50	6.66E+04	7.86	5.24E+05	0.00E+00	0.00E+00	0.00	34	
Inner steel tank, upper part	140.35	137.80	378.18	321.99	1.25E+05	7.86	9.84E+05	0.00E+00	0.00E+00	0.00	35	
Inner steel tank, thick section	140.35	134.60	321.99	261.98	2.98E+05	7.86	2.34E+06	8.62E+01	2.02E+08	0.02	36	1.14E+10
Inner steel tank, lower part	140.35	137.80	261.98	16.52	5.47E+05	7.86	4.30E+06	1.58E+03	6.79E+09	0.57	37	
Bottom plate of inner steel tank	140.35	0.00	16.52	11.44	3.14E+05	7.86	2.47E+06	1.80E+03	4.45E+09	0.37	38	
Bottom plate of lead	151.45	0.00	11.44	1.91	6.87E+05	11.34	7.79E+06	0.00E+00	0.00E+00	0.00	39	
Bottom plate of outer steel tank	151.45	0.00	1.91	0.00	1.38E+05	7.86	1.08E+06	1.07E+03	1.16E+09	0.10	40	2.88E+09
Outer steel tank	151.45	150.50	271.82	16.52	2.30E+05	7.86	1.81E+06	9.52E+02	1.72E+09	0.14	41	
Lead between steel tanks	150.50	140.35	271.82	16.52	2.37E+06	11.34	2.68E+07	0.00E+00	0.00E+00	0.00	42	
Sum							**8.64E+07**		**1.20E+12**	**100.00**		**1.20E+12**

It appears from the figures in Table 1 that the ^{60}Co-activity distribution in the inner construction parts is: reactor tank (5.5%), top shield ring (88.3%), graphite reflector (5.0%), inner steel tank (0.95%) and outer steel tank (0.24%).

3 Dose rates without top shield plug

A model of the inner construction parts of DR 3 that has been used as an input to the Monte Carlo code MCNP5 is based on the information on the dimensions of the inner parts as given in ref. [2]. The graphite reflector has been further subdivided into eleven circular sections and four bottom plates. The model of the inner construction parts is shown in Fig. 1. The model is cylindrical symmetric around the z-axis.

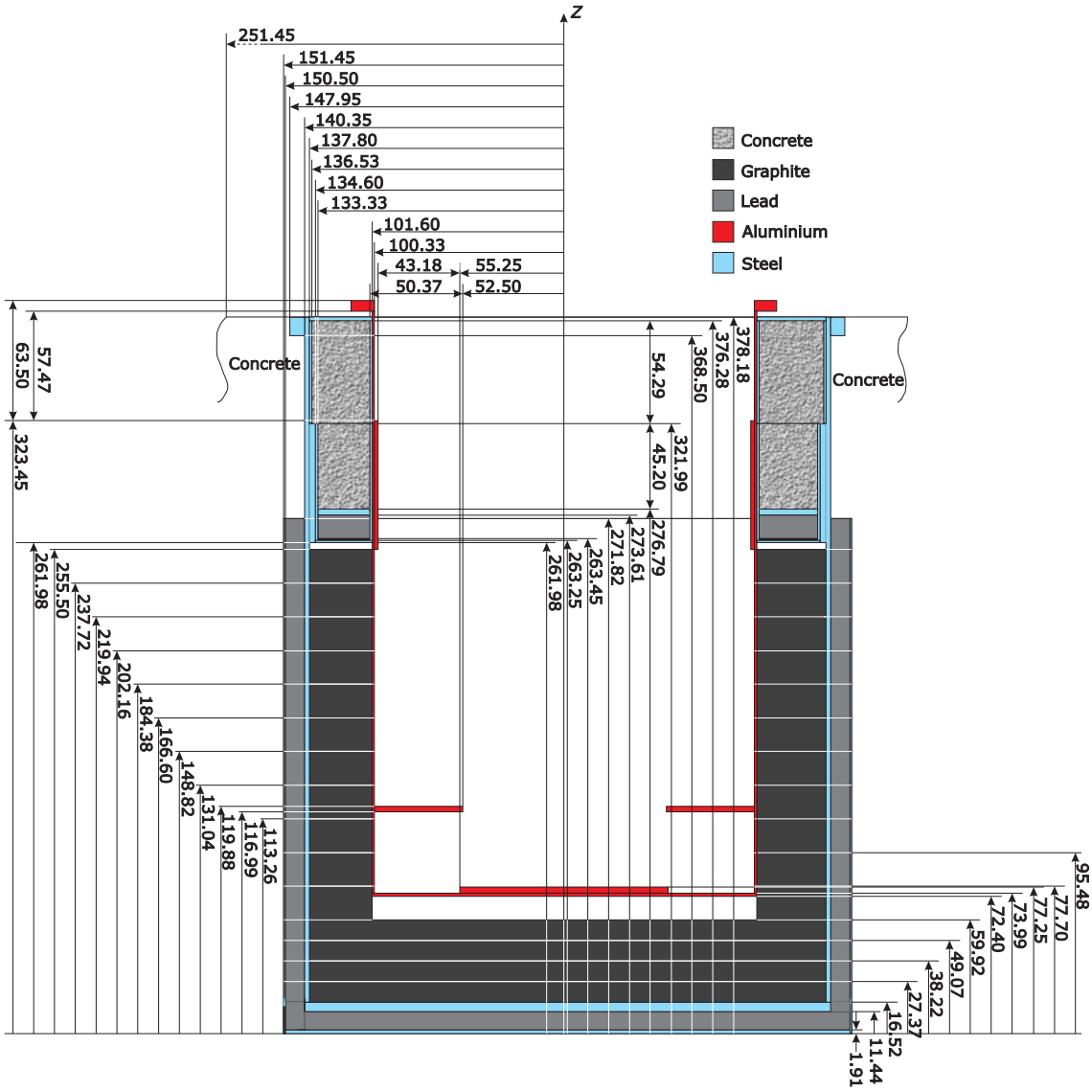

Figure 1. Vertical cross section of the DR 3 model. All dimensions are in cm.

In the model the concrete shield (biological shield) around the inner parts measured from the surface of the outer steel tanks is assumed to be 100 centimeters.

3.1 Dose rates in vertical direction

Calculated γ-dose rate in the centerline of the reactor tank is shown in Fig. 2 for both an empty and a water-filled reactor tank with water up to the bottom of the upper cylinder section (250 centimeters above the tank bottom level).

For the empty reactor tank the maximum dose rate of approximately 100 mSv/h

appears at a distance of about 190 centimeters above the bottom level of the reactor tank. A similar maximum also appears for the water-filled tank. These two maxima are due to the top shield ring containing about 1,000 GBq of ^{60}Co.

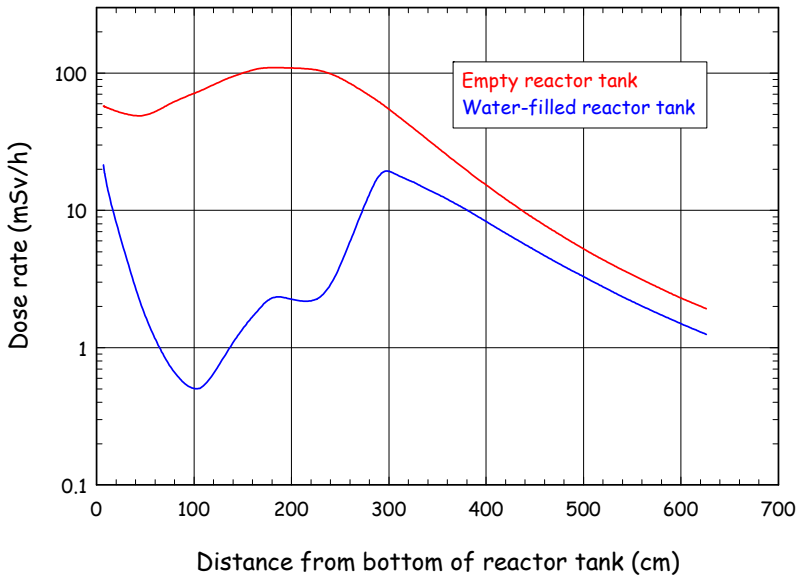

Figure 2. Dose rate from the inner parts of the reactor as a function of vertical distance above the bottom of the reactor tank. The dose rate is calculated at the centerline of an empty reactor tank and a water-filled reactor tank.

For the water-filled reactor tank another maximum of the dose rate appears at a distance of about 300 centimeters above the tank bottom level. As the surface of the water is about 250 centimeters above the tank bottom level, the activity in the thick section of the reactor tank (middle section) is shielded by less and less water seen from a detector point around the 300 centimeter level. Therefore, the activity in the middle reactor tank section will dominate the radiation level here. For increasing detector distances above 300 centimeters the dose rate decreases again as the distance to the source increases.

3.2 Dose rates in horizontal direction

Many operations during the dismantling of the inner parts of the reactor will take place from the top of the reactor. The radiation levels of interest are therefore those in the horizontal range of 0 - 600 centimeters, *i.e.* from the centerline of the reactor tank to about 500 centimeters from the radius of the tank and at a height of about 411 centimeters above the reactor tank bottom (one meter above top level).

The γ-dose rate is calculated for the following situations:

(1) empty reactor tank
(2) water-filled reactor tank
(3) empty reactor tank with a steel ring shielding the top shield ring
(4) water-filled reactor tank with a steel ring shielding the top shield ring

3.2.1 Empty reactor tank

Calculated γ-dose rates are shown in Fig. 3 for different horizontal distances from the tank centerline and for different heights above the tank bottom. It appears from Fig. 3 that the dose rate above the tank opening decreases with height due to increasing distance to the sources. At some distances outside the tank opening the

dose rate increases with height due to decreasing shielding seen from the detector point.

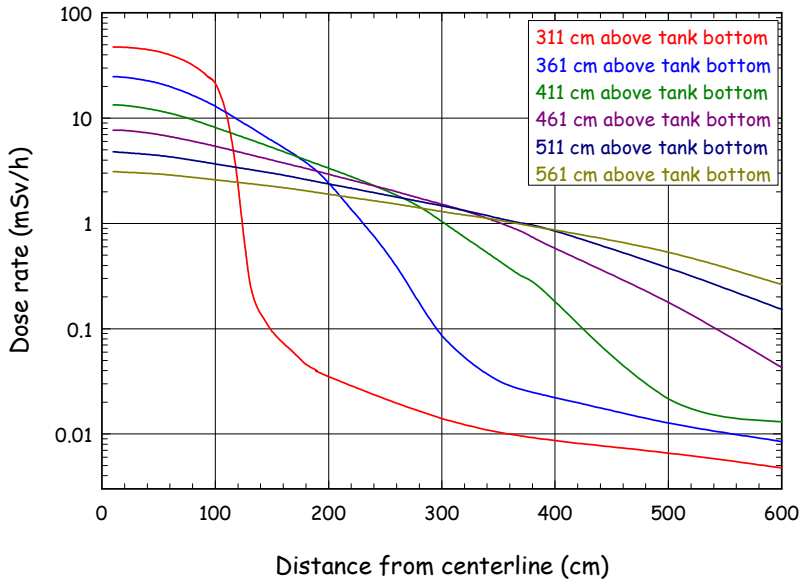

Figure 3. Dose rate from the inner parts of the reactor as a function of horizontal distance from centerline for different vertical distances above the bottom of the reactor tank. The reactor tank is empty.

Selected values from the graphs in Fig. 3 are shown in Table 2.

Table 2. Dose rates in μSv/h from the inner parts of the reactor as a function of horizontal distance from centerline for different vertical distances above the bottom of the reactor tank. The reactor tank is empty.

Vertical distance [cm]	Horizontal distance [cm]						
	10	100	200	300	400	500	600
311	48,000	21,000	35	14	9	7	5
361	25,000	13,000	2,900	86	22	13	8.5
411	13,000	8,200	3,200	1,100	180	22	13
461	7,700	5,400	3,000	1,600	580	180	43
511	4,800	3,700	2,300	1,500	850	380	150
561	3,100	2,600	1,900	1,300	860	530	260

3.2.2 Water-filled reactor tank

Calculated γ-dose rates are shown in Fig. 4 for different horizontal distances from the tank centerline and for different heights above the tank bottom. It appears from Fig. 4 that the dose rate above the tank opening decreases with height, but increases with height at some distances outside the tank opening.

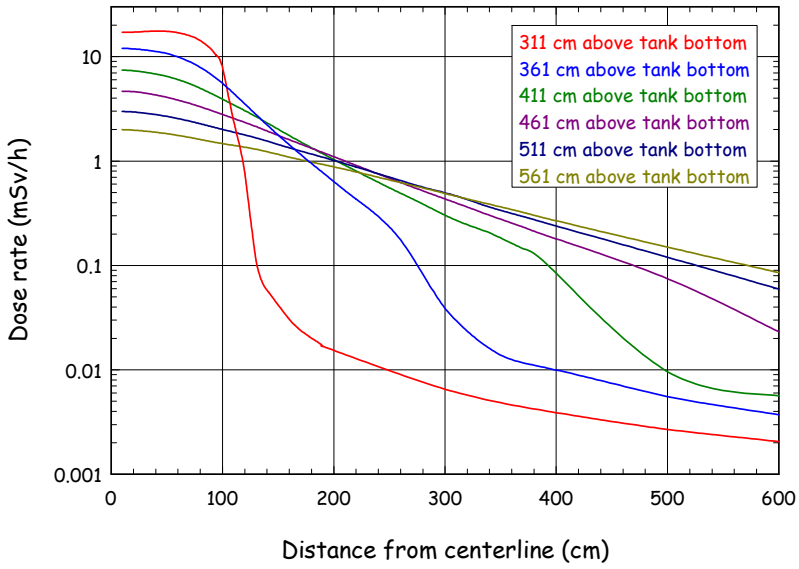

Figure 4. Dose rate from the inner parts of the reactor as a function of horizontal distance from centerline for different vertical distances above the bottom of the reactor tank. The reactor tank contains water up to the top of the middle cylinder section.

Selected values from the graphs in Fig. 4 are shown in Table 3.

Table 3. Dose rates in μSv/h from the inner parts of the reactor as a function of horizontal distance from centerline for different vertical distances above the bottom of the reactor tank. The reactor tank contains water up to the top of the middle cylinder section.

Vertical distance [cm]	Horizontal distance [cm]						
	10	100	200	300	400	500	600
311	17,000	7,900	15	6.5	3.9	2.7	2.1
361	12,000	5,600	700	39	10	5.6	3.7
411	7,400	3,900	1,000	320	85	9.6	5.7
461	4,600	2,800	1,100	420	180	75	23
511	3,000	2,000	1,000	520	240	120	60
561	2,000	1,500	850	490	270	150	86

3.3 Steel ring shields

The activity in the bottom steel plate and inner steel cylinder of the top shield ring can be partly shielded by a steel ring placed concentric within the middle cylinder section of the reactor tank. A steel ring with a weight of 1,900 kg is placed with the ring bottom plane at the bottom plane of the middle cylinder section. The outer diameter of the ring is 96.43 cm, and the air gap between the outer surface of the steel ring and the inner surface of the reactor tank is two

centimeters. For a steel ring mass of 1,900 kg the height and thickness of the ring can be varied as follows:

Height (cm)	Thickness (cm)
40	100
50	79
60	65
70	56

The ring shield would be more effective, *i.e.* a better shielding, if the air gap between the outer surface of the steel ring and the inner surface of the reactor tank were less than two centimeters. However, a tolerance of less than two centimeters would make it difficult to position the steel ring without problems.

3.3.1 Empty reactor tank

Calculated γ-dose rate for an empty reactor tank are shown in Fig. 5 for different steel ring dimensions and different horizontal distances from the tank centerline at a vertical distance above the reactor tank bottom level of 411 centimeters (one meter above the reactor top level).

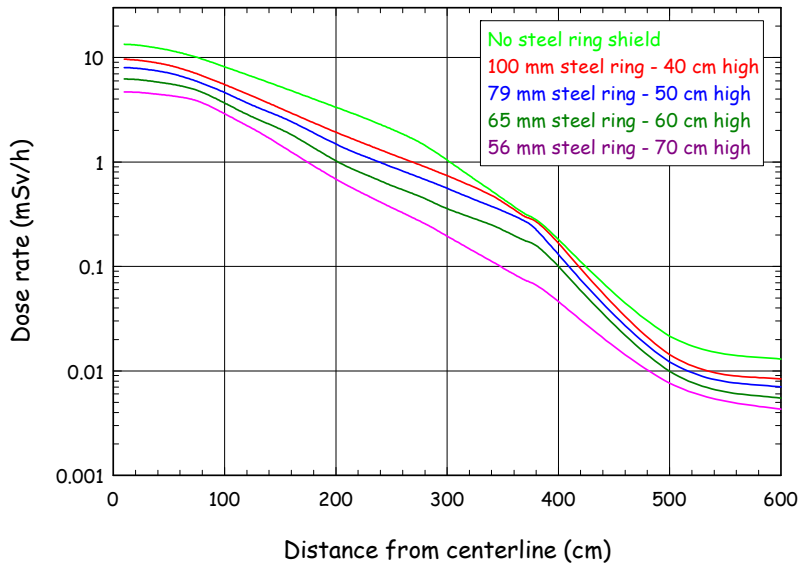

Figure 5. Dose rate from the inner parts of the reactor as a function of horizontal distance from centerline at a vertical distance above the bottom of the reactor tank of 411 cm. The reactor tank is empty. A steel ring with different thickness and height is used as a radiation shield.

It appears from Fig. 5 that a steel ring with height of 70 cm and thickness 56 mm will be the most effective and reduce the radiation level by approximately a factor of 3 - 6 at a distance of 411 cm above the reactor tank bottom level.

Calculated γ-dose rates are shown in Fig. 6 for different horizontal distances from the tank centerline and for different heights above the tank bottom. By comparing Fig. 6 with Fig. 3 it appears that the steel ring will reduce the dose rates at the reactor top from an empty reactor tank by a factor of 2 - 7, depending on the position of the detector point.

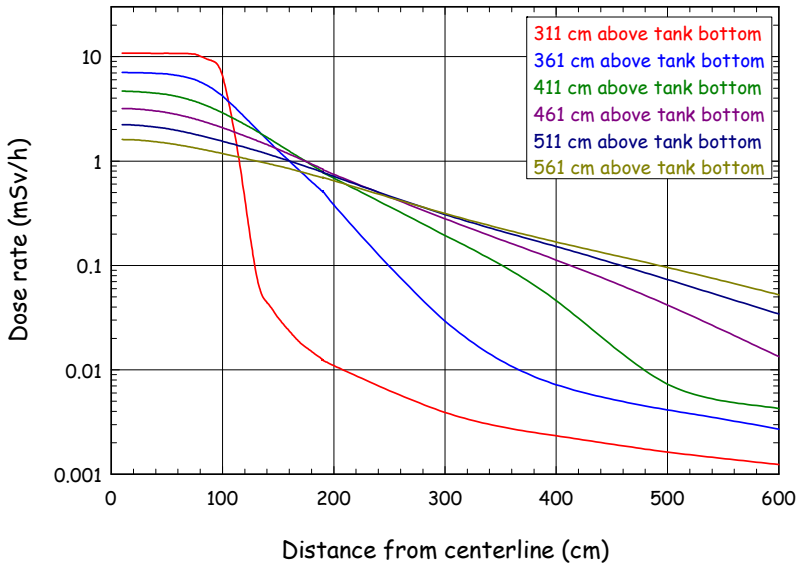

Figure 6. Dose rate from the inner parts of reactor DR 3 as a function of horizontal distance from centerline for different vertical distances above the bottom of the reactor tank. The reactor tank is empty. A steel ring with a thickness of 56 mm and a height of 70 cm is used as a radiation shield.

Selected values from the graphs in Fig. 6 are shown in Table 4.

Table 4. Dose rates in μSv/h from the inner parts of the reactor as a function of horizontal distance from centerline for different distances above the bottom of the reactor tank. The reactor tank is empty. A steel ring with thickness of 56 mm and height of 70 cm is placed with its bottom plane at the bottom of the middle cylinder section.

Vertical distance [cm]	Horizontal distance [cm]						
	10	100	200	300	400	500	600
311	10,800	6,600	11	3.9	2.3	1.6	1.2
361	7,000	4,200	380	29	7.2	4.1	2.7
411	4,700	2,900	690	200	46	7.3	4.3
461	3,200	2,100	750	280	110	42	13
511	2,200	1,600	710	310	150	73	34
561	1,600	1,200	650	320	170	96	53

3.3.2 Water-filled reactor tank

Calculated γ-dose rate for a water-filled reactor tank are shown in Fig. 7 for different steel ring dimensions and different horizontal distances from the tank centerline at a vertical distance above the reactor tank bottom level of 411 centimeters.

It appears from Fig. 7 that a steel ring with height of 70 cm and thickness 56 mm will reduce the radiation level by approximately a factor of 2 - 3 at a distance of 411 cm above the reactor tank bottom.

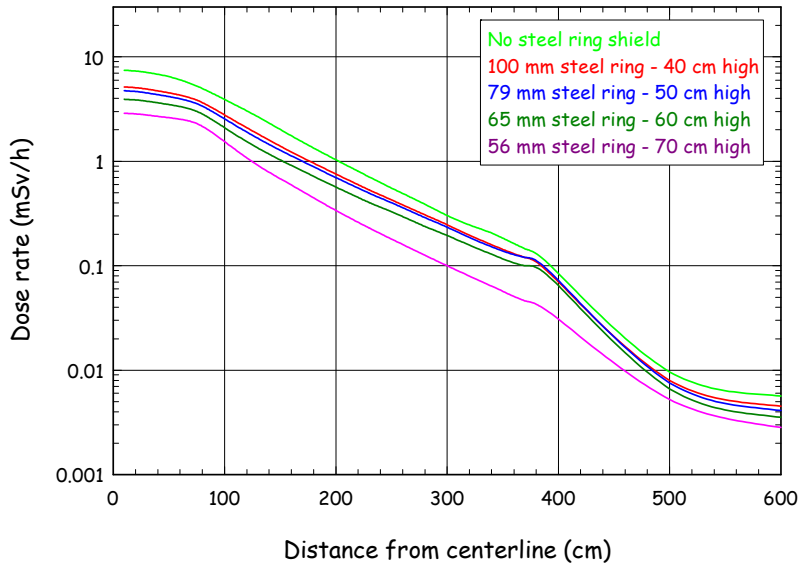

Figure 7. Dose rate from the inner parts of the reactor as a function of horizontal distance from centerline at a vertical distance above the bottom of the reactor tank of 411 cm. The reactor tank contains water up to the top of the middle cylinder section. A steel ring with different thickness and height is used as a radiation shield.

Calculated γ-dose rates are shown in Fig. 8 for different horizontal distances from the tank centerline and for different heights above the tank bottom.

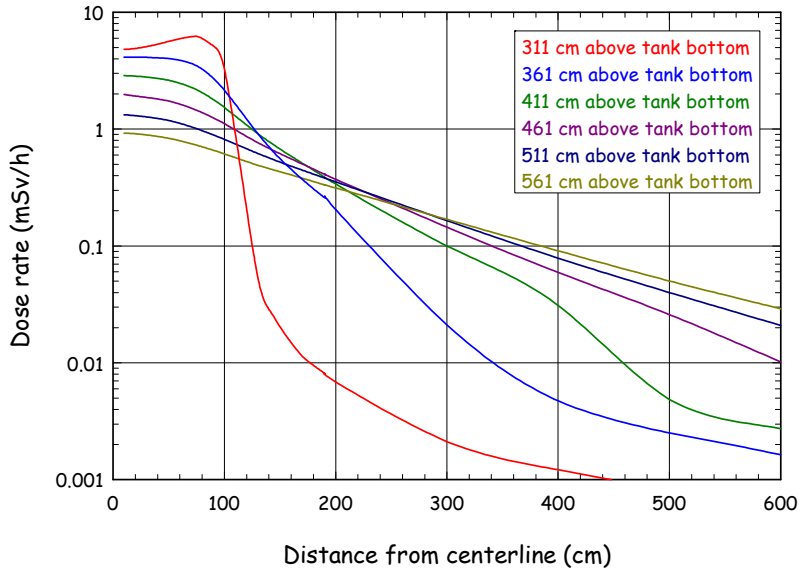

Figure 8. Dose rate from the inner parts of the reactor as a function of horizontal distance from centerline for different vertical distances above the bottom of the reactor tank. The reactor tank contains water up to the top of the middle cylinder section of the reactor tank. A steel ring with a thickness of 56 mm and a height of 70 cm is used as a radiation shield

By comparing Fig. 8 with Fig. 4 it appears that the steel ring will reduce the dose rates at the reactor top from a water-filed reactor tank by a factor of 2 - 4, depending on the position of the detector point. Selected values from the graphs in Fig. 8 are shown in Table 5.

Table 5. Dose rates in μSv/h from the inner parts of the reactor as a function of horizontal distance from centerline for different vertical distances above the bottom of the reactor tank. The tank contains water to the top of the middle cylinder section of the reactor tank. A steel ring with thickness of 56 mm and height of 70 cm is placed with its bottom plane at the bottom of the middle cylinder section.

Vertical distance [cm]	Horizontal distance [cm]						
	10	100	200	300	400	500	600
311	4,800	3,300	6.9	2.1	1.2	0.8	0.6
361	4,100	2,200	200	20	4.7	2.5	1.6
411	2,900	1,500	340	100	31	4.9	2.7
461	2,000	1,100	370	150	60	26	10
511	1,300	820	350	170	80	40	20
561	930	620	300	170	90	50	30

4 Removal of RAT in one piece

The aluminium reactor tank contains about 65 GBq of ^{60}Co. It might be possible to remove the reactor tank in one piece (see Fig. 9) to cut the tank into smaller pieces elsewhere, *e.g.* in the AH-hall. A possibility is to build a concrete shield close to the water pool and successively cut the reactor tank into rings and drop them into the pool for further processing. To evaluate this option, dose rates from an unshielded reactor tank have been calculated and the results presented below.

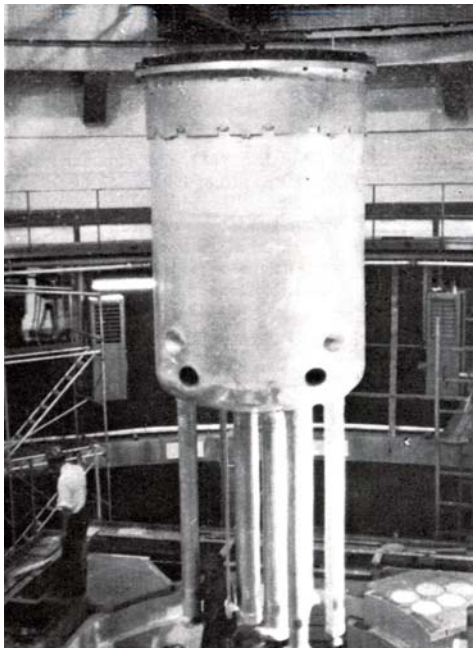

Figure 9. Removal of the reactor tank in one piece. The up- and down-comers might be removed to ease the handling and transport.

4.1 Dose rates outside the reactor tank

Calculated dose rates along the outer surface of the reactor tank at different distances from the surface are shown in Fig. 10. At the surface there are two maxima of the dose rate of about 15 mSv/h at a distance of about 30 cm and 70 cm from the tank bottom level, respectively, due to the contribution from the ^{60}Co-activity in the grid plate and the horizontal experimental tubes.

The dose rate decreases significantly with distance from the tank surface. It appears from Fig. 10 that the dose rate will be reduced to less than 1 mSv/h at distances from the surface of a few metres.

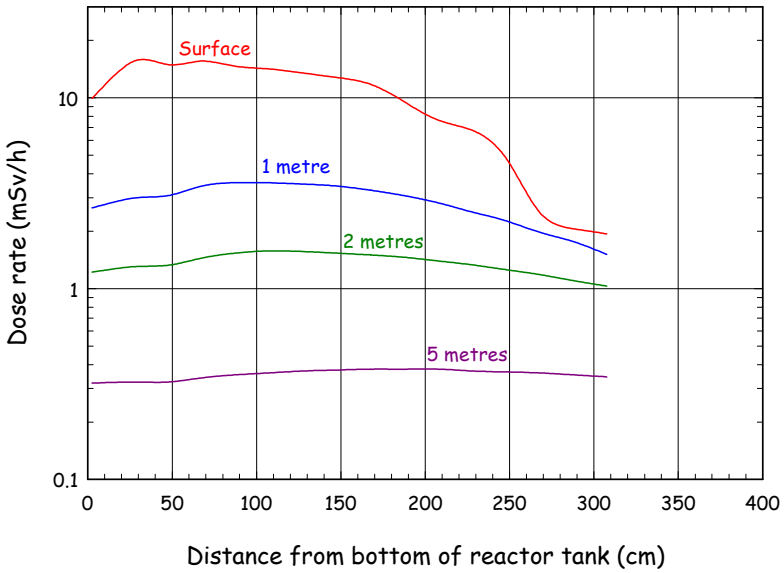

Figure 10. Dose rate along the reactor tank as a function of distance from the bottom of the tank and at different distances from the surface of the tank.

4.2 Dose rates along the reactor tank centerline

Calculated dose rates along the center line of the reactor tank at different distances from the tank bottom - below, inside and above the tank - are shown in Fig. 11.

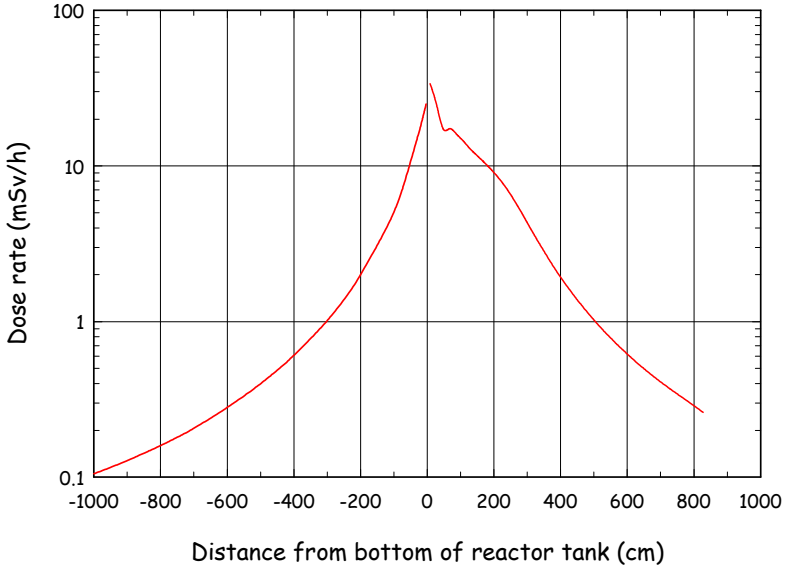

Figure 11. Dose rate along the centerline of the reactor tank as a function of distance from the bottom of the tank.

The dose rate at the tank bottom is about 30 mSv/h and decreases with increasing distance from the bottom. The dose rate decreases more rapidly below the tank bottom as the activity in the tank wall is at a larger distance below than above the tank bottom.

4.3 Comparison with Point Kernel calculations

Earlier, point kernel calculations of the dose rates at the center line of the reactor tank have been made [7]. The dose rates, $\dot{H}(x_0, y_0, z_0)$, at the detector point, (x_0, y_0, z_0), were calculated as:

$$\dot{H}(x_0, y_0, z_0) = \Gamma \cdot \iiint C(x, y, z) \cdot \frac{\exp(-\mu(x, y, z) \cdot r(x, y, z))}{r^2(x, y, z)} \, \mathrm{d}x \, \mathrm{d}y \, \mathrm{d}z$$

where:

- Γ is the exposure rate constant for ^{60}Co
- $r^2(x, y, z) = (x - x_0)^2 + (y - y_0)^2 + (z - z_0)^2$
- $\mu(x, y, z)$ is the linear attenuation coefficient
- $C(x, y, z)$ is the activity concentration around the point (x, y, z)
- $C(x, y, z) \, \mathrm{d}x \, \mathrm{d}y \, \mathrm{d}z$ is the infinitesimal point source at that point

The results of the point kernel calculations are shown in Fig. 12 together with the results of the Monte Carlo calculations.

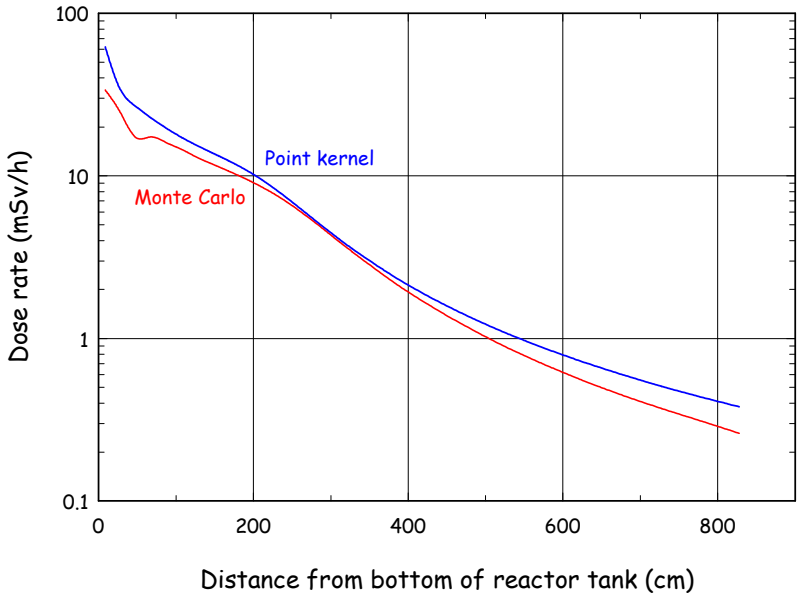

Figure 12. Dose rate along the center line of the reactor tank as a function of distance from the tank bottom calculated with the Monte Carlo and the Point Kernel methods.

Comparing the results from the Monte Carlo and the Point Kernel method shows good agreement. The contribution from scattered photons expressed by the dose build-up factor is not included in the Point Kernel calculations but the dose rates are still somewhat higher than the Monte Carlo results. The reactor tank wall is thin in comparison with the mean free path of the ^{60}Co-photons in aluminium and dose build-up in the Point Kernel calculations would only have increased the calculated dose rates by about 25 - 30%. In addition, absorption of ^{60}Co-photons in the tank wall is not included ($\mu = 0$), which can explain the somewhat higher Point Kernel results.

5 Dose rates without reactor tank but top shield ring present

After the aluminium reactor tank has been removed, the remaining construction parts will be as shown in Fig. 13

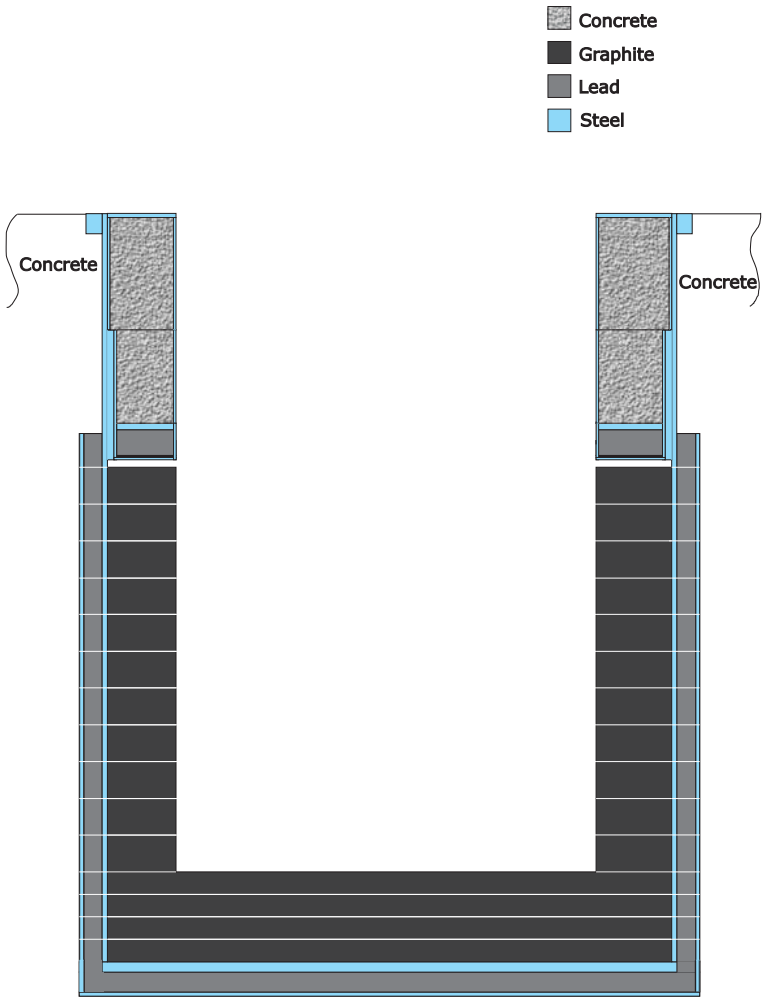

Figure 13. The inner construction parts of DR 3 after removal of the reactor tank are the top shield ring, the graphite reflector, the inner steel tank, lead shield and outer steel tank.

The dominating radiation source will be the bottom steel plate and inner steel cylinder of the top shield ring. The activity distribution in the constructions parts after removal of the reactor tank is given in Table 6. It appears from the figures in the table that the ^{60}Co-activity distribution in the inner construction parts is: top shield ring (93.8%), graphite reflector (5.3%), inner steel tank (1%) and outer steel tank (0.3%).

Table 6. Distribution of activity in the top shield ring, graphite reflector and steel tanks of reactor DR 3.

Construction part	R_o	R_i	H_t	H_b	V	ρ	m	C	Q	Q_{rel}	Cell No.	Q_{part}
	[cm]	[cm]	[cm]	[cm]	[cm^3]	[g/cm^3]	[g]	[Bq/g]	[Bq]	[%]		[Bq]
Top ring, upper part, steel, top	137.80	101.60	378.18	376.28	5.17E+04	7.86	4.07E+05	0.00E+00	0.00E+00	0.00	8	
Top ring, upper part, steel cylinder, outer	137.80	136.53	376.28	321.99	5.94E+04	7.86	4.67E+05	1.35E+02	6.31E+07	5.579E-03	9	
Top ring, upper part, steel cylinder, inner	102.87	101.60	376.28	321.99	4.43E+04	7.86	3.48E+05	2.70E+03	9.40E+08	8.32E-02	10	
Top ring, upper part, shot concrete	136.53	102.87	376.28	321.99	1.37E+06	5.69	7.82E+06	9.80E+00	7.66E+07	6.78E-03	11	
Top ring, lower part, steel cylinder, outer	134.60	133.33	321.99	263.25	6.28E+04	7.86	4.94E+05	4.43E+04	2.19E+10	1.93	12	1.06E+12
Top ring, lower part, steel cylinder, inner	102.87	101.60	321.99	263.25	4.79E+04	7.86	3.77E+05	8.85E+05	3.33E+11	29.49	13	
Top ring, lower part, shot concrete	133.33	102.87	321.99	276.79	1.02E+06	5.69	5.81E+06	8.96E+02	5.21E+09	0.46	14	
Top ring, lower part, steel plates	133.33	102.87	276.79	273.61	7.19E+04	7.86	5.65E+05	4.55E+03	2.57E+09	0.23	15	
Top ring, lower part, lead	133.33	102.87	273.61	263.45	2.30E+05	11.34	2.60E+06	1.18E+01	3.07E+07	0.00	16	
Top ring, lower part, cadmium	133.33	102.87	263.45	263.25	4.52E+03	8.64	3.91E+04	0.00E+00	0.00E+00	0.00	17	
Top ring, lower part, steel plate bottom	134.60	101.60	263.25	261.98	3.11E+04	7.86	2.44E+05	2.83E+06	6.92E+11	61.21	18	
Graphite, 1st radial layer from top	137.80	101.60	261.98	237.72	6.61E+05	2.20	1.45E+06	3.37E+03	4.90E+09	0.43	19	
Graphite, 2nd radial layer from top	137.80	101.60	237.72	219.94	4.84E+05	2.20	1.06E+06	3.37E+03	3.59E+09	0.32	20	
Graphite, 3rd radial layer from top	137.80	101.60	219.94	202.16	4.84E+05	2.20	1.06E+06	3.37E+03	3.59E+09	0.32	21	
Graphite, 4th radial layer from top	137.80	101.60	202.16	184.38	4.84E+05	2.20	1.06E+06	3.37E+03	3.59E+09	0.32	22	
Graphite, 5th radial layer from top	137.80	101.60	184.38	166.60	4.84E+05	2.20	1.06E+06	3.37E+03	3.59E+09	0.32	23	
Graphite, 6th radial layer from top	137.80	101.60	166.60	148.82	4.84E+05	2.20	1.06E+06	3.37E+03	3.59E+09	0.32	24	
Graphite, 7th radial layer from top	137.80	101.60	148.82	131.04	4.84E+05	2.20	1.06E+06	3.37E+03	3.59E+09	0.32	25	
Graphite, 8th radial layer from top	137.80	101.60	131.04	113.26	4.84E+05	2.20	1.06E+06	3.37E+03	3.59E+09	0.32	26	6.00E+10
Graphite, 9th radial layer from top	137.80	101.60	113.26	95.48	4.84E+05	2.20	1.06E+06	3.37E+03	3.59E+09	0.32	27	
Graphite, 10th radial layer from top	137.80	101.60	95.48	77.70	4.84E+05	2.20	1.06E+06	3.37E+03	3.59E+09	0.32	28	
Graphite, 11th radial layer from top	137.80	101.60	77.70	59.92	4.84E+05	2.20	1.06E+06	3.37E+03	3.59E+09	0.32	29	
Graphite, bottom layer, 1st layer from top	137.80	0.00	59.92	49.07	6.47E+05	2.20	1.42E+06	3.37E+03	4.80E+09	0.42	30	
Graphite, bottom layer, 2nd layer from top	137.80	0.00	49.07	38.22	6.47E+05	2.20	1.42E+06	3.37E+03	4.80E+09	0.42	31	
Graphite, bottom layer, 3rd layer from top	137.80	0.00	38.22	27.37	6.47E+05	2.20	1.42E+06	3.37E+03	4.80E+09	0.42	32	
Graphite, bottom layer, 4th layer from top	137.80	0.00	27.37	16.52	6.47E+05	2.20	1.42E+06	3.37E+03	4.80E+09	0.42	33	
Inner steel tank, top flange	147.95	140.35	378.18	368.50	6.66E+04	7.86	5.24E+05	0.00E+00	0.00E+00	0.00	34	
Inner steel tank, upper part	140.35	137.80	378.18	321.99	1.25E+05	7.86	9.84E+05	0.00E+00	0.00E+00	0.00	35	
Inner steel tank, thick section	140.35	134.60	321.99	261.98	2.98E+05	7.86	2.34E+06	8.62E+01	2.02E+08	0.02	36	1.14E+10
Inner steel tank, lower part	140.35	137.80	261.98	16.52	5.47E+05	7.86	4.30E+06	1.58E+03	6.79E+09	0.60	37	
Bottom plate of inner steel tank	140.35	0.00	16.52	11.44	3.14E+05	7.86	2.47E+06	1.80E+03	4.45E+09	0.39	38	
Bottom plate of lead	151.45	0.00	11.44	1.91	6.87E+05	11.34	7.79E+06	0.00E+00	0.00E+00	0.00	39	
Bottom plate of outer steel tank	151.45	0.00	1.91	0.00	1.38E+05	7.86	1.08E+06	1.07E+03	1.16E+09	0.10	40	2.88E+09
Outer steel tank	151.45	150.50	271.82	16.52	2.30E+05	7.86	1.81E+06	9.52E+02	1.72E+09	0.15	41	
Lead between steel tanks	150.50	140.35	271.82	16.52	2.37E+06	11.34	2.68E+07	0.00E+00	0.00E+00	0.00	42	
Sum							**8.51E+07**		**1.13E+12**	**100.00**		**1.13E+12**

5.1 Dose rates in horizontal direction

Calculated dose rates in the horizontal direction at the top of the reactor without the reactor tank are shown in Fig. 14.

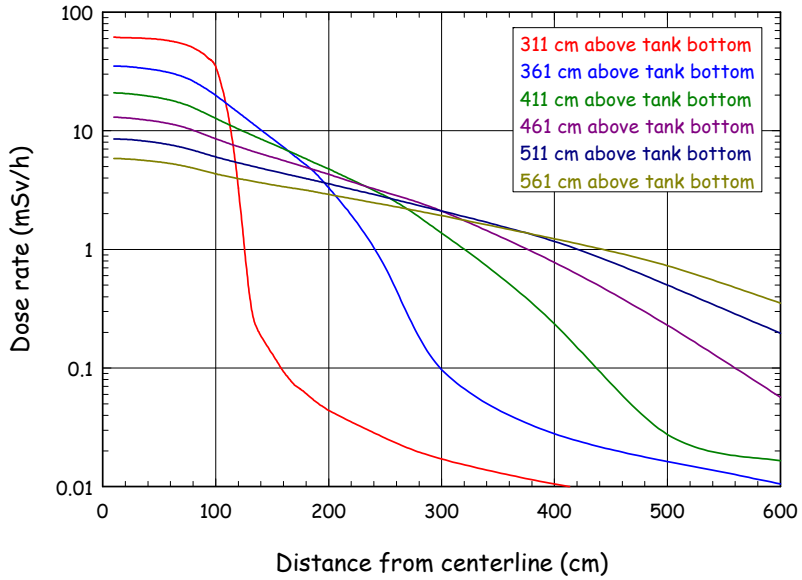

Figure 14. Dose rate from the inner parts of the reactor as a function of horizontal distance from centerline without reactor tank. The detector points are placed 1 meter above the top floor, i.e. 411 cm above the tank bottom level.

By comparing Fig. 14 and Fig. 3 it appears that the dose rates increase when the reactor tank has been removed. This is because the middle cylinder section of the reactor tank shields the activity in the inner steel cylinder of the lower part of the top shield ring. Selected values from the graphs in Fig. 14 are shown in Table 7.

Table 7. Dose rates in μSv/h from the inner parts of the reactor as a function of horizontal distance from centerline for different vertical distances above the bottom of the reactor tank. The reactor tank is removed.

Vertical distance [cm]	Horizontal distance [cm]						
	10	100	200	300	400	500	600
311	62,000	35,000	44	17	11	8	6
361	35,000	20,000	3,300	100	28	16	11
411	21,000	13,000	4,800	1,400	240	28	17
461	13,000	8,600	4,300	2,100	780	230	57
511	8,500	6,000	3,600	2,100	1,200	500	200
561	5,900	4,300	2,900	1,900	1,200	730	350

5.2 Dose rates in vertical direction

Calculated dose rates in the vertical direction along the centerline of the reactor without the reactor tank (and with reactor tank for comparison) are shown in Fig. 15.

It appears from Fig. 15 that the dose rate in the centerline increases slightly when the reactor tank is removed. Again, the reason is that the shielding effect of the reactor tank more than counterbalances the radiation from the removed activity in the reactor tank.

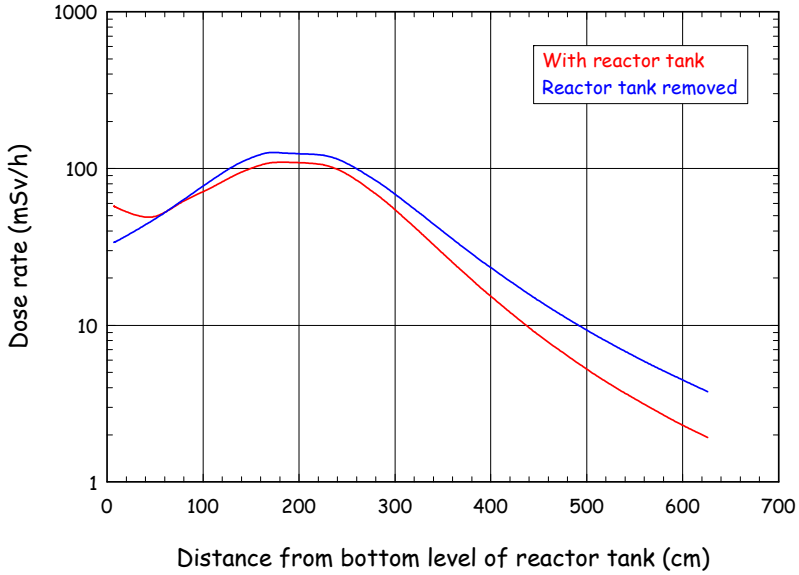

Figure 15. Dose rate from the inner parts of the reactor as a function of vertical distance above the bottom of the reactor tank. The dose rate is calculated at the centerline of the reactor with and without reactor tank.

6 Removal of RAT in sections without top shield ring

If the aluminium reactor tank is removed after the top shield ring is removed, an option is to remove the tank in sections by cutting operations from the top of the reactor. The RAT-sections are removed in the following order:

- upper cylinder section
- middle cylinder section
- horizontal experimental tubes
- lower sections (lower cylinder section, bottom cylinder and bottom plate)

These sections of the reactor tank are assumed to be removed from an empty tank or from a water-filled tank with a water level up to the bottom af the section being removed.

6.1 Tank cutting with empty reactor tank

Calculated dose rates at the top af the reactor are shown in Fig. 16.

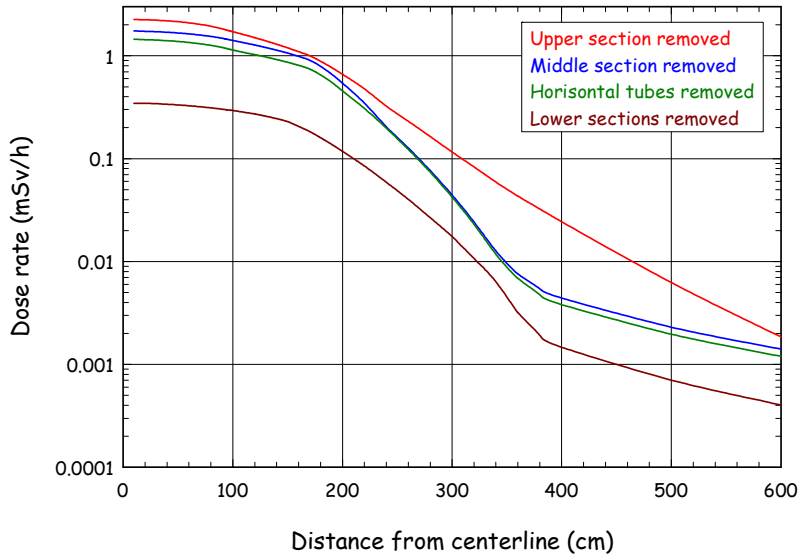

Figure 16. Dose rate from the inner parts of the reactor as a function of horizontal distance from centerline without top shield ring. The reactor tank is removed in sections. The detector points are placed 1 meter above the top floor, i.e. 411 cm above the tank bottom level.

Selected values from the graphs in Fig. 16 are shown in Table 8.

Table 8. Dose rates in μSv/h from the inner parts of the reactor as a function of horizontal distance from centerline without top shield ring. The reactor tank is removed in sections. The detector points are placed 1 meter above the top floor, i.e. 411 cm above the tank bottom level.

Tank component removed	Horizontal distance [cm]						
	10	100	200	300	400	500	600
Upper section	2,300	1,700	660	110	25	6	2
Middle section	1,700	1,400	540	45	4	2	1
Horizontal tubes	1,400	1,100	450	40	4	2	1
Lower section	350	300	120	18	1.5	0.7	0.4

The reduction in dose rate at the top of the reactor following the removal of the different sections is about 5 - 10 from beginning to end.

The calculated dose rate along the centerline of the tank is shown in Fig. 17. At the bottom level of the tank the dose rate is reduced significantly following the removal of the different sections of the tank. After all the tank sections have been removed, the bottom dose rate is reduced by a factor of about 10.

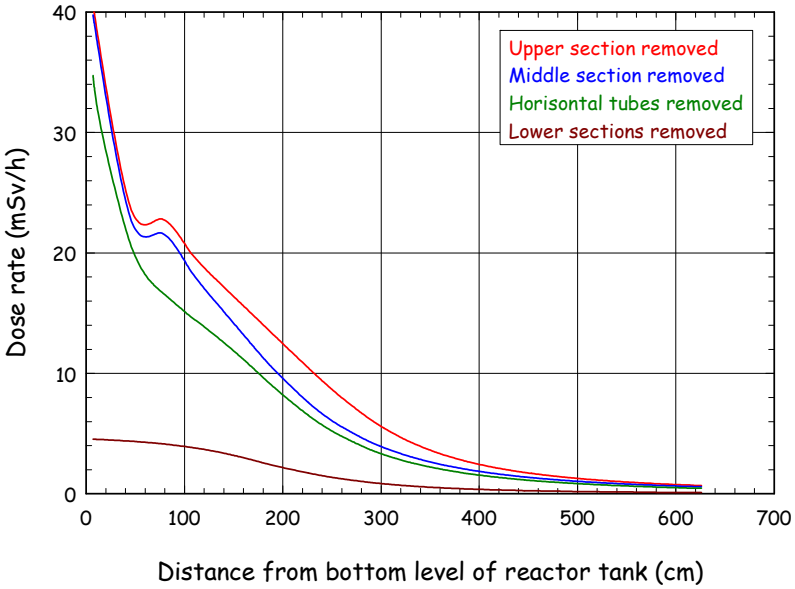

Figure 17. Dose rate along the centerline of the reactor tank as a function of vertical distance from the reactor tank bottom without top shield ring. The reactor tank is removed in sections.

6.2 Tank cutting with water-filled reactor tank

Calculated dose rates at the top af the reactor are shown in Fig. 18 for a water-filled tank during removal of the different tank sections.

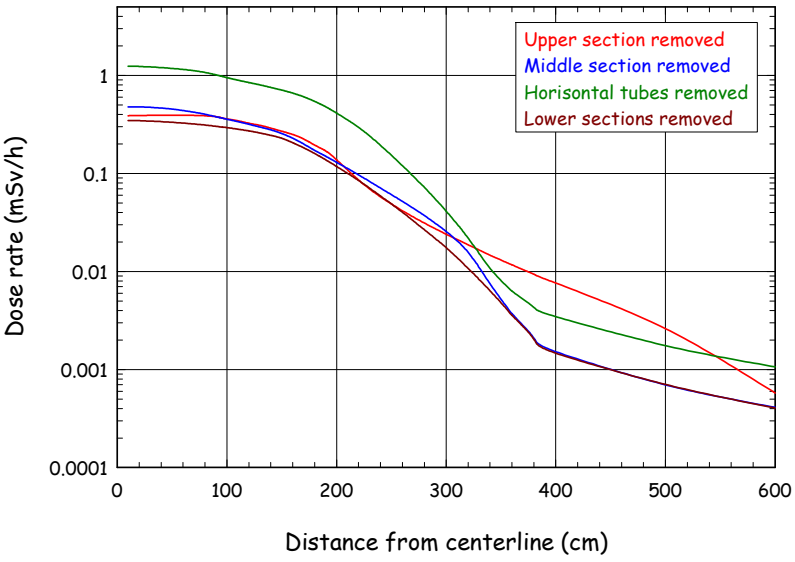

Figure 18. Dose rate from the inner parts of the reactor as a function of horizontal distance from centerline without top shield ring. The reactor tank is removed in sections and the tank is filled with water up to the bottom of the section being removed. The detector points are placed 1 meter above the top floor, i.e. 411 cm above the tank bottom level.

Selected values from the graphs in Fig. 18 are shown in Table 9.

Table 9. Dose rates in μSv/h from the inner parts of the reactor as a function of horizontal distance from centerline without top shield ring. The reactor tank is removed in sections and the tank is filled with water up to the bottom of the section being removed. The detector points are placed 1 meter above the top floor, i.e. 411 cm above the tank bottom level.

Tank component removed	Horizontal distance [cm]						
	10	100	200	300	400	500	600
Upper section	400	360	140	24	8	2.6	0.6
Middle section	480	360	130	26	1.5	0.7	0.4
Horizontal tubes	1,200	1,000	400	40	3.5	1.8	1.1
Lower section	350	300	120	18	1.5	0.7	0.4

The calculated dose rate along the centerline of the tank is shown in Fig. 19 for a water-filled reactor tank up to the bottom of the tank section being removed. After removal of the upper and middle sections, the dose rates have maximum values at a distance of about 300 and 240 centimeters above the tank bottom, respectively.

After the RAT upper section has been removed, the middle sections of the reactor tank and inner steel tank are still shielded by water. A maximum dose rate appears about 50 cm above the water level where the shielding-distance effect is optimal. When the middle RAT section has been removed, the middle section of the inner steel tank becomes unshielded. The activity in this part of the steel tank therefore dominates the dose rate. For increasing distances along the centerline, the dose rates decrease again as the distance to the source increases.

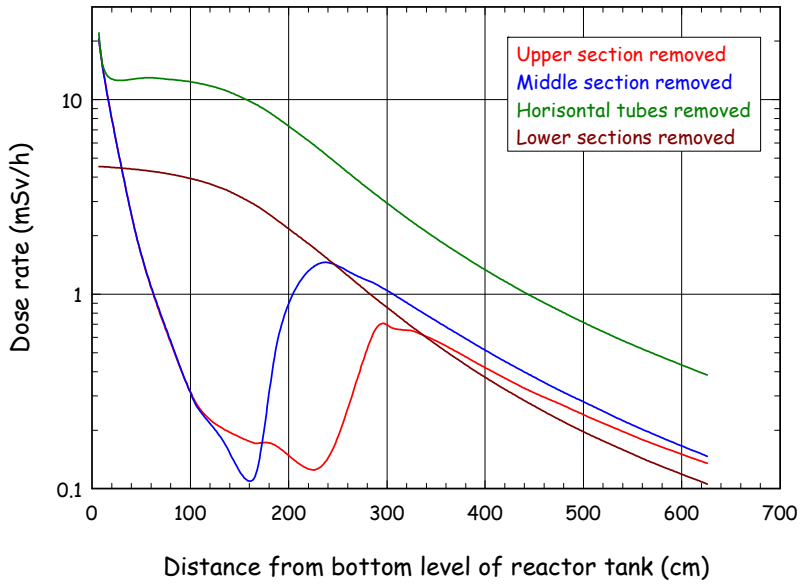

Figure 19. Dose rate along the centerline of the reactor tank as a function of vertical distance from the reactor tank bottom without top shield ring. The reactor tank is removed in sections and the tank is filled with water up to the bottom of the section being removed.

By comparing Fig. 18 with Fig. 16 it appears that the dose rates at the reactor top from a water-filled reactor tank is smaller than the corresponding dose rates from an empty reactor tank, but the difference decreases as the water level is decreased.

6.3 Tank cutting with sand-filled reactor tank

Calculated dose rates at the top af the reactor are shown in Fig. 20 for a sand-filled tank during removal of the different tank sections.

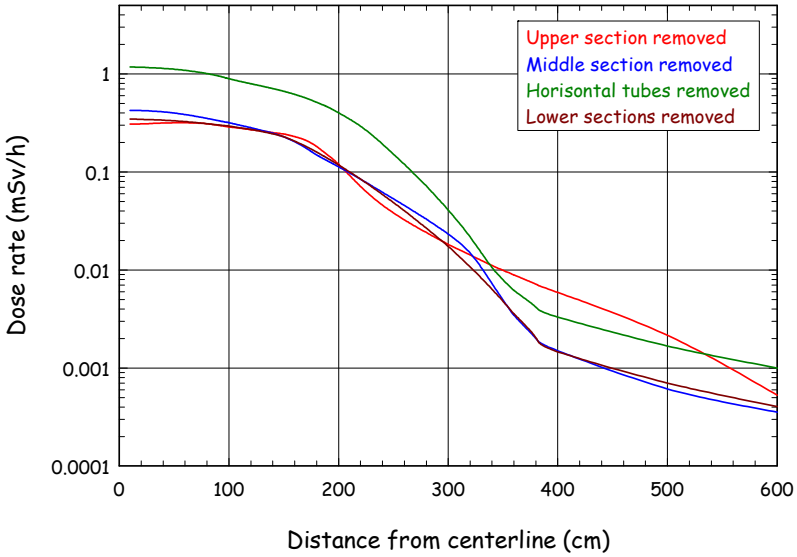

Figure 20. Dose rate from the inner parts of the reactor as a function of horizontal distance from centerline without top shield ring. The reactor tank is removed in sections and the tank is filled with sand up to the bottom of the section being removed. The detector points are placed 1 meter above the top floor, i.e. 411 cm above the tank bottom level.

Selected values from the graphs in Fig. 20 are shown in Table 10.

Table 10. Dose rates in μSv/h from the inner parts of the reactor as a function of horizontal distance from centerline without top shield ring. The reactor tank is removed in sections and the tank is filled with sand up to the bottom of the section being removed. The detector points are placed 1 meter above the top floor, i.e. 411 cm above the tank bottom level.

Tank component removed	Horizontal distance [cm]						
	10	100	200	300	400	500	600
Upper section	310	290	120	18	5.9	2.2	0.5
Middle section	430	320	110	23	1.5	0.6	0.4
Horizontal tubes	1,200	900	400	40	3.3	1.7	1.0
Lower section	350	300	120	18	1.5	0.7	0.4

Comparing Fig. 20 with Fig. 18 shows that the dose rates with a water-filled reactor tank are only marginal higher than with a sand-filled reactor tank.

7 Dose rates without top shield ring and reactor tank

After the top shield ring an the reactor tank have been removed the remaining construction parts are as shown in Fig. 21.

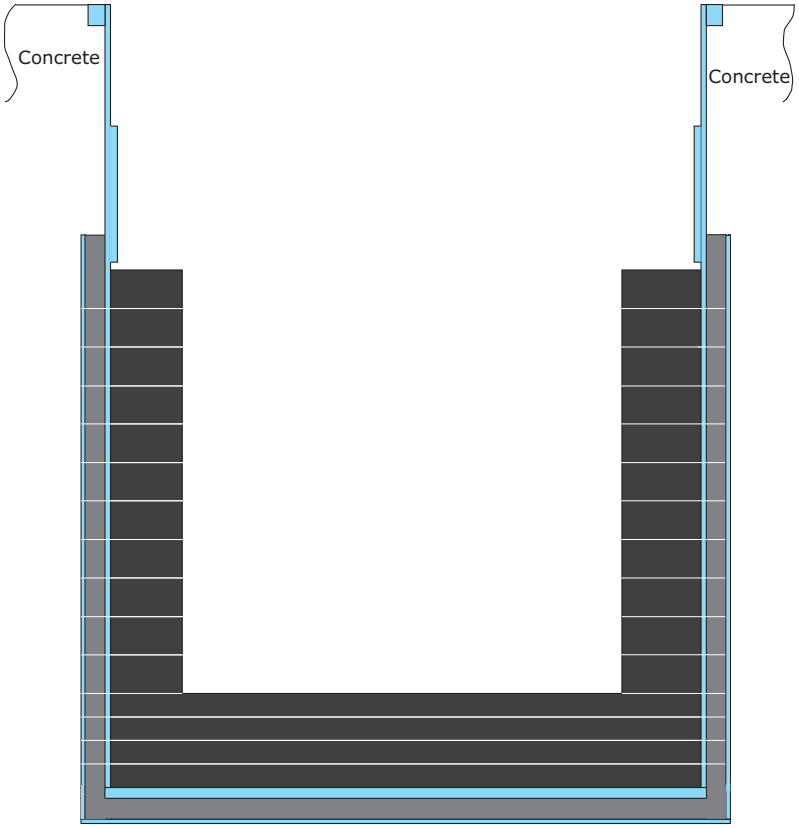

Figure 21. The inner construction parts of DR 3 after removal of the reactor tank and the top shield ring are the graphite reflector, the inner steel tank, lead shield and outer steel tank.

The activity distribution in the constructions parts after removal of the reactor tank and top shield ring is given in Table 11. It appears from the figures in the table that the ^{60}Co-activity distribution in the inner construction parts is: graphite reflector (81%), inner steel tank (15%) and outer steel tank (4%).

The dismantling of the graphite reflector and the steel tanks can be carried out vertically from the top of the reactor or horizontally from outside in. The γ-dose rates from the steel tanks and graphite reflector have therefore been calculated for the following three situations:

(1) inside and above the graphite and steel tanks

(2) along the steel tanks and graphite with a concrete shield

(3) along the steel tanks and graphite without shielding ('naked' steel tanks)

If the steel tanks and the graphite reflector are dismantled from the side of the steel tanks and not from the reactor top, some shielding of the tanks and graphite would be necessary. The biological shield around the steel tanks could be removed and about 30 centimeters be left to act as a shield.

Table 11. Distribution of activity in the graphite reflector and steel tanks of reactor DR 3.

Construction part	R_o	R_i	H_t	H_b	V	ρ	m	C	Q	Q_{rel}	Cell No.	Q_{part}
	[cm]	[cm]	[cm]	[cm]	[cm^3]	[g/cm^3]	[g]	[Bq/g]	[Bq]	[%]		[Bq]
Graphite, 1st radial layer from top	137.80	101.60	261.98	237.72	6.61E+05	2.20	1.45E+06	3.37E+03	4.90E+09	6.59	19	6.00E+10
Graphite, 2nd radial layer from top	137.80	101.60	237.72	219.94	4.84E+05	2.20	1.06E+06	3.37E+03	3.59E+09	4.83	20	
Graphite, 3rd radial layer from top	137.80	101.60	219.94	202.16	4.84E+05	2.20	1.06E+06	3.37E+03	3.59E+09	4.83	21	
Graphite, 4th radial layer from top	137.80	101.60	202.16	184.38	4.84E+05	2.20	1.06E+06	3.37E+03	3.59E+09	4.83	22	
Graphite, 5th radial layer from top	137.80	101.60	184.38	166.60	4.84E+05	2.20	1.06E+06	3.37E+03	3.59E+09	4.83	23	
Graphite, 6th radial layer from top	137.80	101.60	166.60	148.82	4.84E+05	2.20	1.06E+06	3.37E+03	3.59E+09	4.83	24	
Graphite, 7th radial layer from top	137.80	101.60	148.82	131.04	4.84E+05	2.20	1.06E+06	3.37E+03	3.59E+09	4.83	25	
Graphite, 8th radial layer from top	137.80	101.60	131.04	113.26	4.84E+05	2.20	1.06E+06	3.37E+03	3.59E+09	4.83	26	
Graphite, 9th radial layer from top	137.80	101.60	113.26	95.48	4.84E+05	2.20	1.06E+06	3.37E+03	3.59E+09	4.83	27	
Graphite, 10th radial layer from top	137.80	101.60	95.48	77.70	4.84E+05	2.20	1.06E+06	3.37E+03	3.59E+09	4.83	28	
Graphite, 11th radial layer from top	137.80	101.60	77.70	59.92	4.84E+05	2.20	1.06E+06	3.37E+03	3.59E+09	4.83	29	
Graphite, bottom layer, 1st layer from top	137.80	0.00	59.92	49.07	6.47E+05	2.20	1.42E+06	3.37E+03	4.80E+09	6.46	30	
Graphite, bottom layer, 2nd layer from top	137.80	0.00	49.07	38.22	6.47E+05	2.20	1.42E+06	3.37E+03	4.80E+09	6.46	31	
Graphite, bottom layer, 3rd layer from top	137.80	0.00	38.22	27.37	6.47E+05	2.20	1.42E+06	3.37E+03	4.80E+09	6.46	32	
Graphite, bottom layer, 4th layer from top	137.80	0.00	27.37	16.52	6.47E+05	2.20	1.42E+06	3.37E+03	4.80E+09	6.46	33	
Inner steel tank, top flange	147.95	140.35	378.18	368.50	6.66E+04	7.86	5.24E+05	0.00E+00	0.00E+00	0.00	34	1.14E+10
Inner steel tank, upper part	140.35	137.80	378.18	321.99	1.25E+05	7.86	9.84E+05	0.00E+00	0.00E+00	0.00	35	
Inner steel tank, thick section	140.35	134.60	321.99	261.98	2.98E+05	7.86	2.34E+06	8.62E+01	2.02E+08	0.27	36	
Inner steel tank, lower part	140.35	137.80	261.98	16.52	5.47E+05	7.86	4.30E+06	1.58E+03	6.79E+09	9.14	37	
Bottom plate of inner steel tank	140.35	0.00	16.52	11.44	3.14E+05	7.86	2.47E+06	1.80E+03	4.45E+09	5.99	38	
Bottom plate of lead	151.45	0.00	11.44	1.91	6.87E+05	11.34	7.79E+06	0.00E+00	0.00E+00	0.00	39	2.88E+09
Bottom plate of outer steel tank	151.45	0.00	1.91	0.00	1.38E+05	7.86	1.08E+06	1.07E+03	1.16E+09	1.56	40	
Outer steel tank	151.45	150.50	271.82	16.52	2.30E+05	7.86	1.81E+06	9.52E+02	1.72E+09	2.32	41	
Lead between steel tanks	150.50	140.35	271.82	16.52	2.37E+06	11.34	2.68E+07	0.00E+00	0.00E+00	0.00	42	
Sum							**6.59E+07**		**7.43E+10**	**100.00**		**7.43E+10**

7.1 Dose rates inside and above the graphite and steel tanks

Calculated γ-dose rates are shown in Fig. 22 for different horizontal distances from the tank centerline and for different heights above the tank bottom.

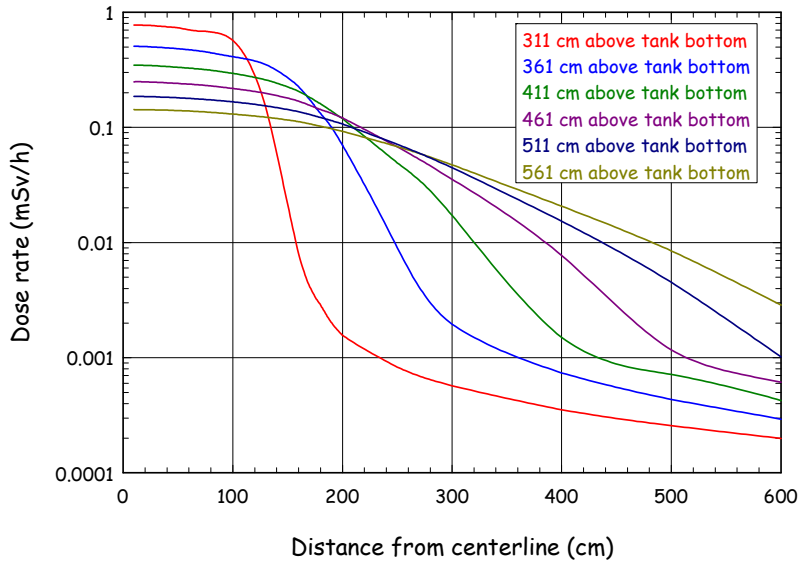

Figure 22. Dose rate from the inner parts of the reactor as a function of horizontal distance from centerline without reactor tank and top shield ring. The detector points are placed at different vertical distances above the bottom level of the reactor tank.

Selected values from the graphs in Fig. 22 are shown in Table 12.

Table 12. Dose rates in μSv/h from the inner parts of the reactor as a function of horizontal distance from centerline without reactor tank and top shield ring. The detector points are placed at different vertical distances above the bottom level of the reactor tank.

Vertical distance [cm]	Horizontal distance [cm]						
	10	100	200	300	400	500	600
311	780	570	1.6	0.6	0.4	0.3	0.2
361	500	410	70	2	0.7	0.4	0.3
411	350	300	120	17	1.5	0.7	0.4
461	250	220	120	35	8	1	0.6
511	190	170	100	45	15	5	1
561	140	130	90	50	20	8	3

Calculated γ-dose rates along the centerline of the reactor are shown in Fig. 23.

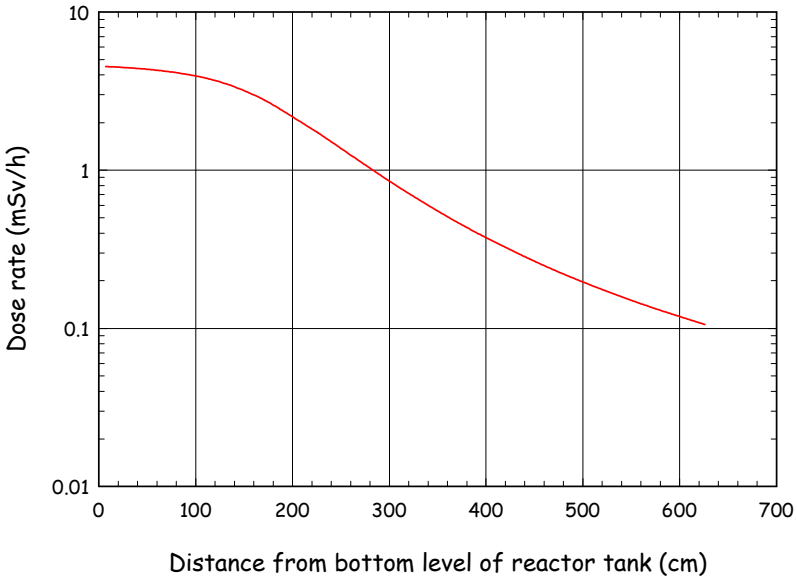

Figure 23. Dose rate from the inner parts of the reactor as a function of vertical distance above the bottom level of the reactor tank. The dose rate is calculated at the centerline of the reactor without reactor tank and top shield ring.

7.2 Dose rates along the steel tanks and graphite

The dismantling of the graphite and steel tanks might be carried out from the side of the steel tanks after the major part of or all the biological shield has been removed. The geometries for the calculations is shown Fig. 24.

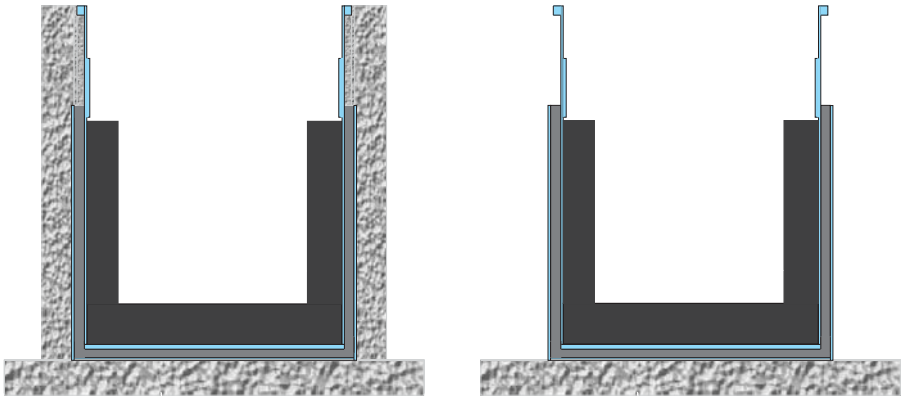

Figure 24. Dismantling of the biological concrete shield around the steel tanks and graphite reflector. Radiation levels are calculated for a 30 cm concrete shield around the steel tanks and for the steel tanks without shielding.

Calculated γ-dose rates are shown in Fig. 25 for shielded steel tanks as a function of vertical distance above the steel tank bottom and for different horizontal distances from the surface of the concrete shield.

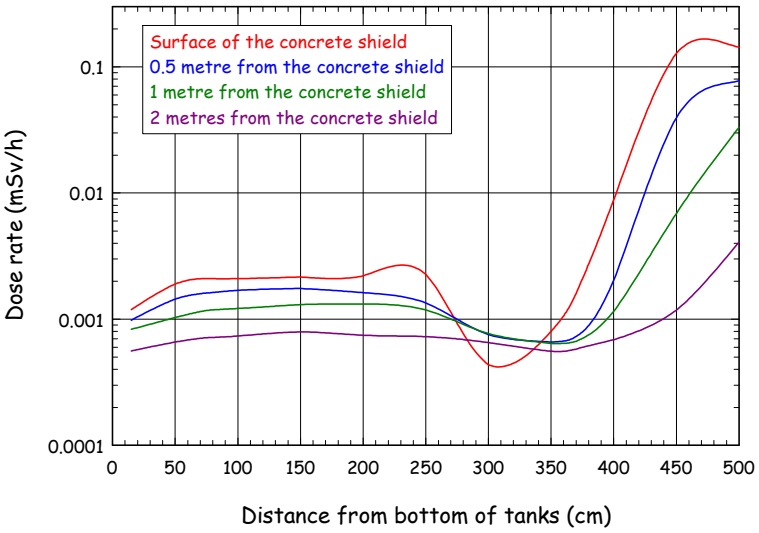

Figure 25. Dose rate from the steel tanks and graphite reflector as a function of vertical distance above the bottom of the tanks. The steel tanks are shielded by 30 cm of the biological concrete shield. The detector points are placed at different horizontal distances from the surface of the concrete shield.

Selected values from the graphs in Fig. 25 are shown in Table 13.

Table 13. Dose rates in μSv/h from the steel tanks and graphite reflector as a function of vertical distance from the bottom of the tanks. The steel tanks are shielded by 30 cm of the biological concrete shield. The detector points are placed at different horizontal distances from the surface of the concrete shield.

Horizontal distance [cm]	Vertical distance [cm]						
	15	100	200	300	350	400	500
0	1.2	2.1	2.2	0.4	0.8	9	140
50	1	1.7	1.6	0.8	0.7	2	78
100	0.8	1.2	1.3	0.8	0.6	1.2	33
200	0.6	0.7	0.7	0.7	0.6	0.7	4

It appears from Fig. 25 that the γ-dose rates in the vertical direction - depending on the horizontal distance - are 1 - 2 μSv/h up to a height of about 350 centimeters above the steel tank bottom. If the height is increased, the dose rates increase significantly because the upper part of the steel tanks and graphite become unshielded.

Calculated γ-dose rates are shown in Fig. 26 for unshielded steel tanks as a function of vertical distance above the steel tank bottom and for different horizontal distances from the surface of the outer steel tank.

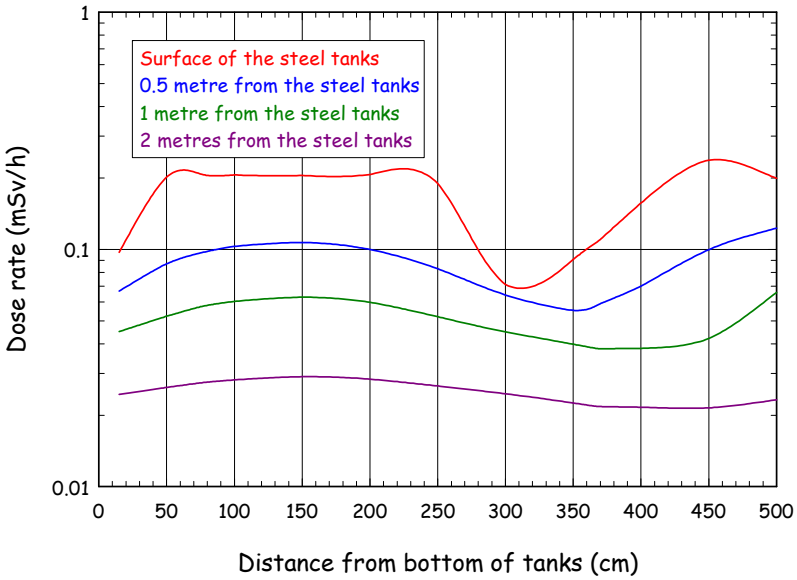

Figure 26. Dose rate from the steel tanks and graphite reflector as a function of vertical distance from the bottom of the tanks. The steel tanks are unshielded. The detector points are placed at different horizontal distances from the surface of the bare outer steel tank.

Selected values from the graphs in Fig. 26 are shown in Table 14.

Table 14. Dose rates in μSv/h from the steel tanks and graphite reflector as a function of vertical distance from the bottom of the tanks. The steel tanks are unshielded. The detector points are placed at different horizontal distances from the surface of the bare tanks.

Horizontal distance [cm]	Vertical distance [cm]						
	15	100	200	300	350	400	500
0	100	210	210	70	90	160	200
50	70	100	100	65	55	70	120
100	45	60	60	45	40	40	65
200	25	30	30	25	23	22	23

It appears from Fig. 26 that the γ-dose rates in the vertical directions - depending on the horizontal distance - are 20 - 200 μSv/h up to a height of 500 centimeters above the steel tank bottom.

8 Removal of graphite reflector

In the model, the graphite reflector has been subdivided into eleven radial layers and four bottom layers as shown in Fig. 1 at page 3. It is here assumed that the graphite reflector is removed from operations at the top of the reactor.

8.1 Dose rates in horizontal direction

Calculated γ-dose rates are shown in Fig. 27 for different horizontal distances from the tank centerline and at a height of 411 centimeters above the reactor tank bottom level.

It appears from Fig. 27 that the γ-dose rates decrease as the different graphite layers are removed. At working places on the reactor top the dose rate is up to about 100 - 300 μSv/h before the removal of the graphite begins.

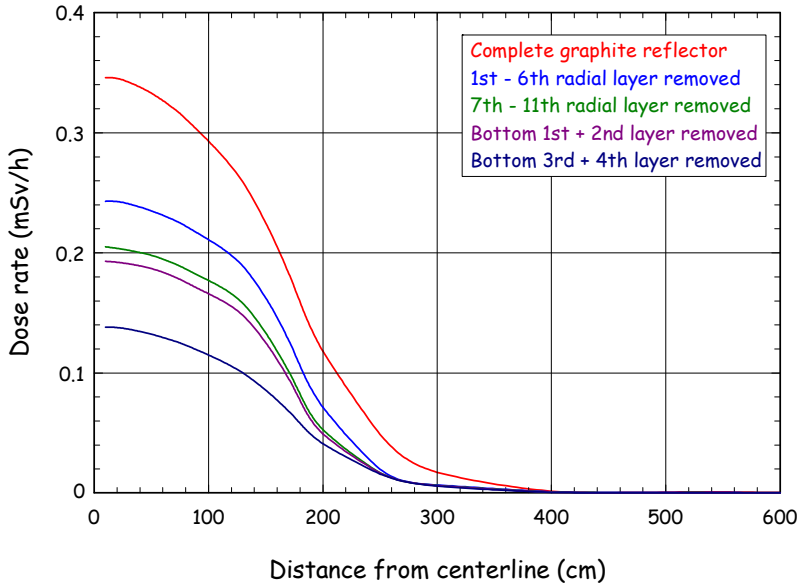

Figure 27. Dose rate from the inner parts of the reactor as a function of horizontal distance from centerline and with different parts of the graphite reflector removed. The detector points are placed 1 meter above the top floor, i.e. 411 cm above the reactor tank bottom level.

Selected values from the graphs in Fig. 27 are shown in Table 15.

Table 15. Dose rates in μSv/h from the inner parts of the reactor as a function of horizontal distance from centerline and with different parts of the graphite reflector removed. The detector points are placed 1 meter above the top floor, i.e. 411 cm above the reactor tank bottom level. The graphite is removed in sections.

Graphite component removed	Horizontal distance [cm]						
	10	100	200	300	400	500	600
Graphite present	350	290	120	17	1.5	0.7	0.4
Radial layer 1 - 6	240	210	70	6.7	1.0	0.4	0.2
Radial layer 7 - 11	200	180	53	6.3	0.8	0.4	0.2
Bottom layer 1 - 2	190	170	50	6.2	0.8	0.3	0.2
Bottom layer 3 - 4	140	120	40	5.8	0.6	0.3	0.1

8.2 Dose rates in vertical direction

Calculated γ-dose rates along the centerline of the reactor are shown in Fig. 28. The upper graph is identical to the graph in Fig. 23 at page 24 and the lower graph in Fig. 17 at page 18. After the graphite has been removed, the γ-dose rate at the bottom level of the reactor tank has decreased by a factor of about 3.

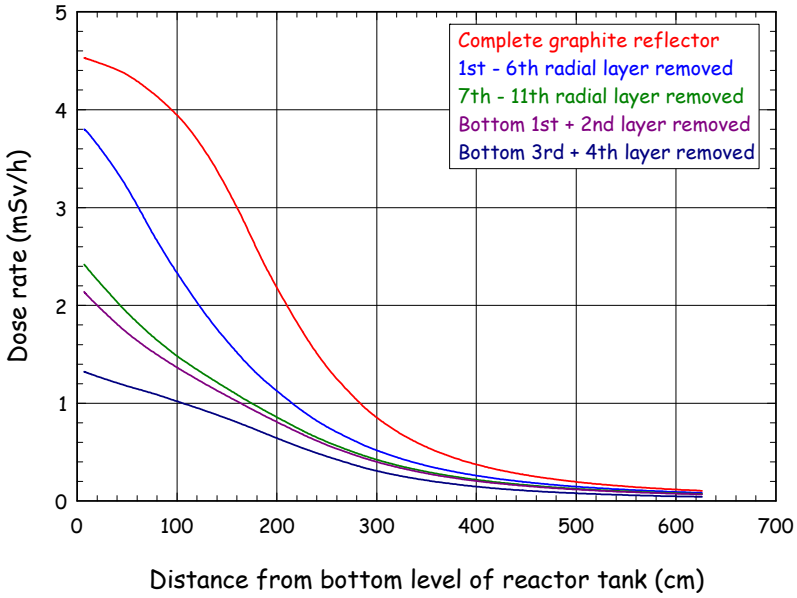

Figure 28. Dose rate from the inner parts of the reactor as a function of vertical distance above the bottom level of the reactor tank. The dose rate is calculated at the centerline of the reactor with different parts of the graphite reflector removed.

9 Removal of inner steel tank

After the graphite reflector has been removed, the dose rate at the top floor of the reactor originates from the activity in the two steel tanks shown in Fig. 29. The dismantling of the steel tanks can be carried out vertically from the top of the reactor or horizontally from the side of the steel tanks.

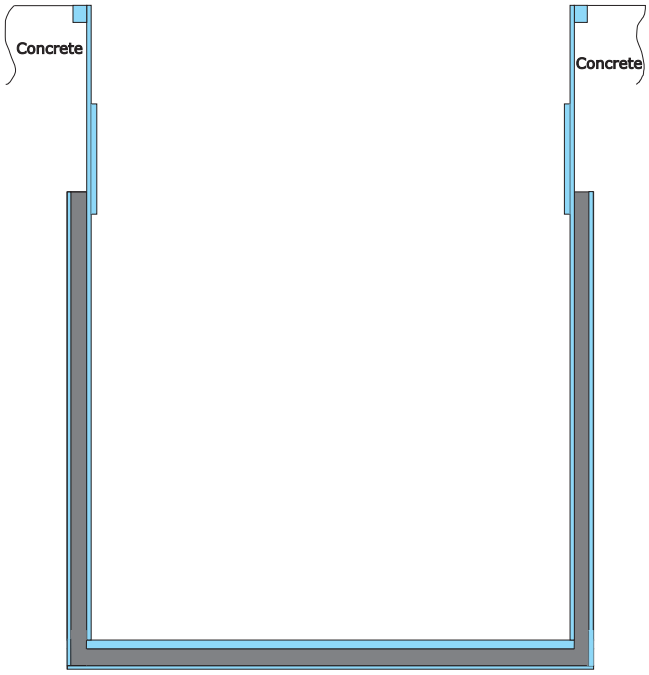

Figure 29. The inner construction parts after removal of the top shield ring, the reactor tank and the graphite reflector are the inner and outer steel tanks.

The activity distribution in the steel tanks after removal of the graphite reflector is given in Table 16. The ^{60}Co-activity distribution in the steel tanks is: inner steel tank (80%) and outer steel tank (20%).

Table 16. Distribution of activity in the steel tanks of reactor DR 3.

Construction part	R_o	R_i	H_t	H_b	V	ρ	m	C	Q	Q_{rel}	Cell No.	Q_{part}
	[cm]	[cm]	[cm]	[cm]	[cm^3]	[g/cm^3]	[g]	[Bq/g]	[Bq]	[%]		[Bq]
Inner steel tank, top flange	147.95	140.35	378.18	368.50	6.66E+04	7.86	5.24E+05	0.00E+00	0.00E+00	0.00	34	1.14E+10
Inner steel tank, upper part	140.35	137.80	378.18	321.99	1.25E+05	7.86	9.84E+05	0.00E+00	0.00E+00	0.00	35	
Inner steel tank, thick section	140.35	134.60	321.99	261.98	2.98E+05	7.86	2.34E+06	8.62E+01	2.02E+08	1.41	36	
Inner steel tank, lower part	140.35	137.80	261.98	16.52	5.47E+05	7.86	4.30E+06	1.58E+03	6.79E+09	47.43	37	
Bottom plate of inner steel tank	140.35	0.00	16.52	11.44	3.14E+05	7.86	2.47E+06	1.80E+03	4.45E+09	31.06	38	
Bottom plate of lead	151.45	0.00	11.44	1.91	6.87E+05	11.34	7.79E+06	0.00E+00	0.00E+00	0.00	39	2.88E+09
Bottom plate of outer steel tank	151.45	0.00	1.91	0.00	1.38E+05	7.86	1.08E+06	1.07E+03	1.16E+09	8.08	40	
Outer steel tank	151.45	150.50	271.82	16.52	2.30E+05	7.86	1.81E+06	9.52E+02	1.72E+09	12.02	41	
Lead between steel tanks	150.50	140.35	271.82	16.52	2.37E+06	11.34	2.68E+07	0.00E+00	0.00E+00	0.00	42	
Sum							**4.81E+07**		**1.43E+10**	**100.00**		**1.43E+10**

9.1 Dose rates inside and above the steel tanks

The γ-dose rates from the steel tanks have been calculated in the horizontal direction and shown in Fig. 30 for different horizontal distances from the tank centerline at a height of 411 centimeters above the reactor tank bottom level and for different parts of the inner steel tank removed.

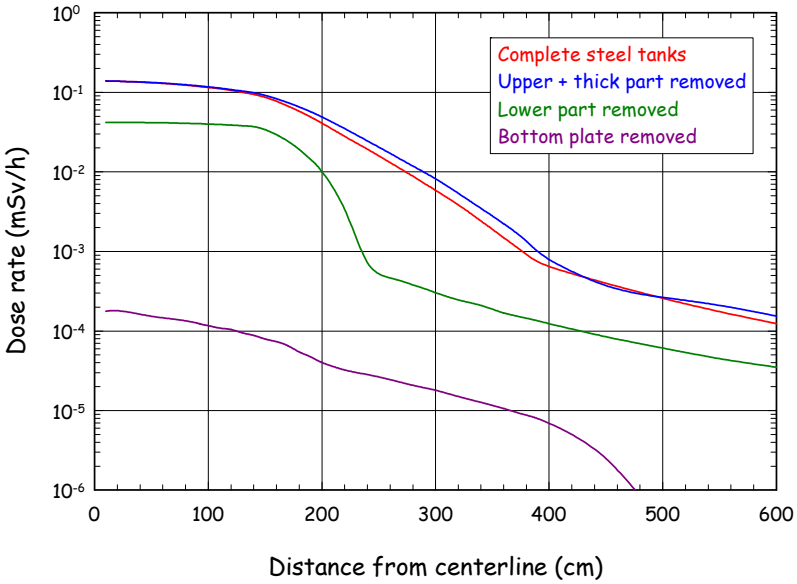

Figure 30. Dose rate from the inner parts of the reactor as a function of horizontal distance from centerline and with different parts of the inner steel tank removed. The detector points are placed 1 meter above the top floor, i.e. 411 cm above the removed aluminium tank bottom level.

Selected values from the graphs in Fig. 30 are shown in Table 17.

Table 17. Dose rates in μSv/h from the steel tanks at a height of 411 cm above the reactor tank bottom level and at different horizontal distances from the tank centerline. The inner steel tank is removed in sections.

Tank component removed	Horizontal distance [cm]						
	10	100	200	300	400	500	600
Tank present	140	120	40	5.8	0.6	0.3	0.1
Upper + thick part	140	120	50	8.2	0.8	0.3	0.2
Lower part	42	40	10	0.3	0.1	0.06	0.04
Bottom plate	0.18	0.12	0.04	0.02	0.007	0.0004	0.0002

Calculated γ-dose rates along the centerline of the reactor are shown in Fig. 31.

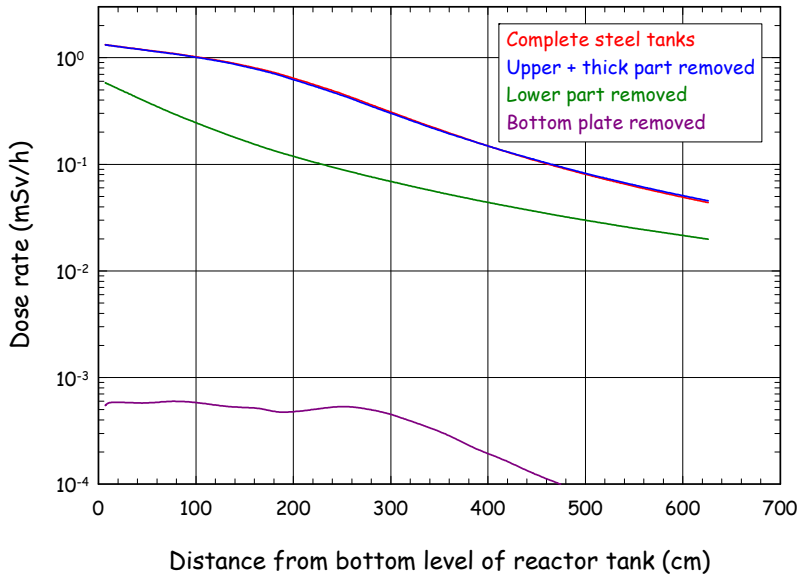

Figure 31. Dose rate from the inner parts of the reactor as a function of vertical distance above the bottom level of the reactor tank. The dose rate is calculated at the centerline of the reactor with different parts of the inner steel tank removed.

9.2 Dose rates along the steel tanks

The dismantling of the steel tanks might be carried out from the side of the steel tanks after the major part of the of or all the biological shield has been removed. The geometry for the calculations is shown in Fig. 32.

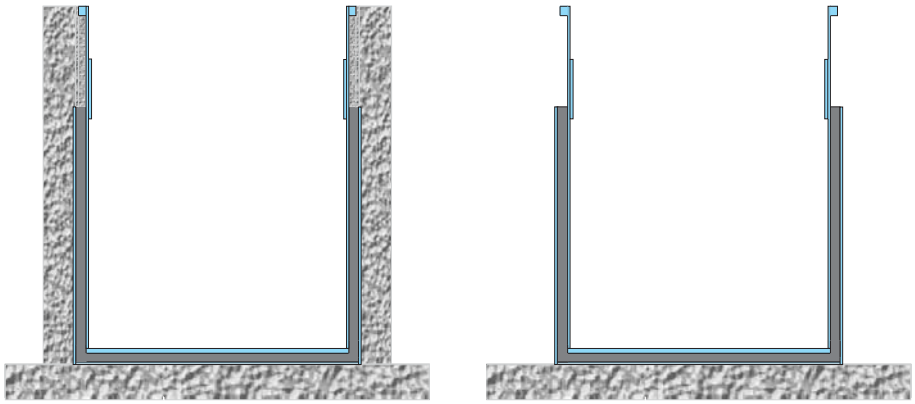

Figure 32. Dismantling of the biological concrete shield around the steel tanks. Radiation levels are calculated for a 30 cm concrete shield around the steel tanks and for the steel tanks without shielding.

Calculated γ-dose rates are shown in Fig. 33 for shielded steel tanks as a function of vertical distance above the steel tank bottom and for different horizontal distances from the surface of the concrete shield.

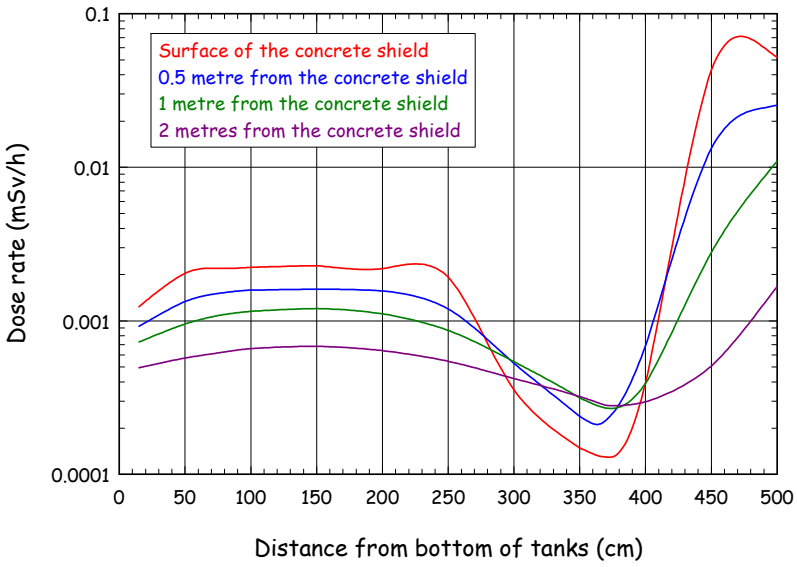

Figure 33. Dose rate from the steel tanks as a function of vertical distance from the bottom of the tanks. The steel tanks are shielded by 30 cm of the biological concrete shield. The detector points are placed at different horizontal distances from the surface of the concrete shield.

Selected values from the graphs in Fig. 33 are shown in Table 18.

Table 18. Dose rates in μSv/h from the steel tanks as a function of vertical distance from the bottom of the tanks. The steel tanks are shielded by 30 cm of the biological concrete shield. The detector points are placed at different horizontal distances from the surface of the concrete shield.

Horizontal distance [cm]	Vertical distance [cm]						
	15	100	200	300	350	400	500
0	1.2	2.2	2.2	0.4	0.2	0.4	50
50	0.9	1.6	1.6	0.5	0.2	0.7	25
100	0.7	1.1	1.1	0.5	0.3	0.4	11
200	0.5	0.7	0.6	0.4	0.3	0.3	1.7

It appears from Fig. 33 that the γ-dose rates in the vertical direction - depending on the horizontal distance - are 0.2 - 2 μSv/h up to a height of about 400 centimeters above the steel tank bottom. If the height is increased, the dose rates increase significantly because the upper part of the steel tanks and graphite become unshielded.

Comparing Fig. 33 with Fig. 25 at page 25 shows that the γ-dose rates at heights of 450 - 500 centimeters at the surface plane of the concrete shield for the steel tanks alone are approximately 2 - 3 times lower than for the steel tanks and graphite reflector. This is due to the contribution to the dose rate from the upper part of the graphite reflector at these heights.

Calculated γ-dose rates are shown in Fig. 34 for unshielded steel tanks as a function of vertical distance above the steel tank bottom and for different horizontal distances from the surface of the outer steel tank.

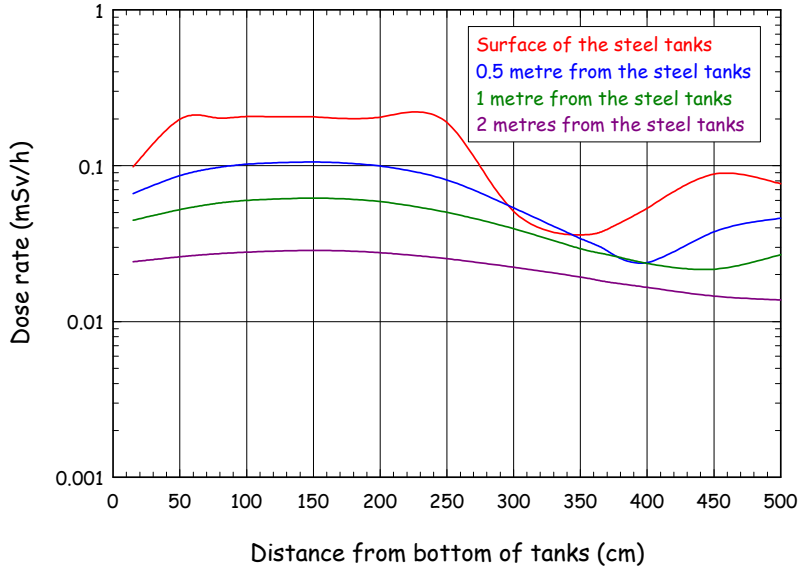

Figure 34. Dose rate from the steel tanks as a function of vertical distance from the bottom of the tanks. The steel tanks are unshielded. The detector points are placed at different horizontal distances from the surface of the bare tanks.

Selected values from the graphs in Fig. 34 are shown in Table 19.

Table 19. Dose rates in μSv/h from the steel tanks as a function of vertical distance from the bottom of the tanks. The steel tanks are unshielded. The detector points are placed at different horizontal distances from the surface of the bare tanks.

Horizontal distance [cm]	Vertical distance [cm]						
	15	100	200	300	350	400	500
0	100	200	200	51	36	53	77
50	66	100	100	54	34	24	46
100	45	60	59	39	29	24	27
200	24	28	28	22	19	17	14

9.3 Sideways removal of the steel tanks

According to Table 18 and Table 19 the dose rates along the steel tanks are moderate, even without a concrete shield. Therefore, the steel tanks might be dismantled sideways, *i.e.* the biological concrete shield around the tanks can be removed partly or completely without a significant increase of the radiation level around the tanks.

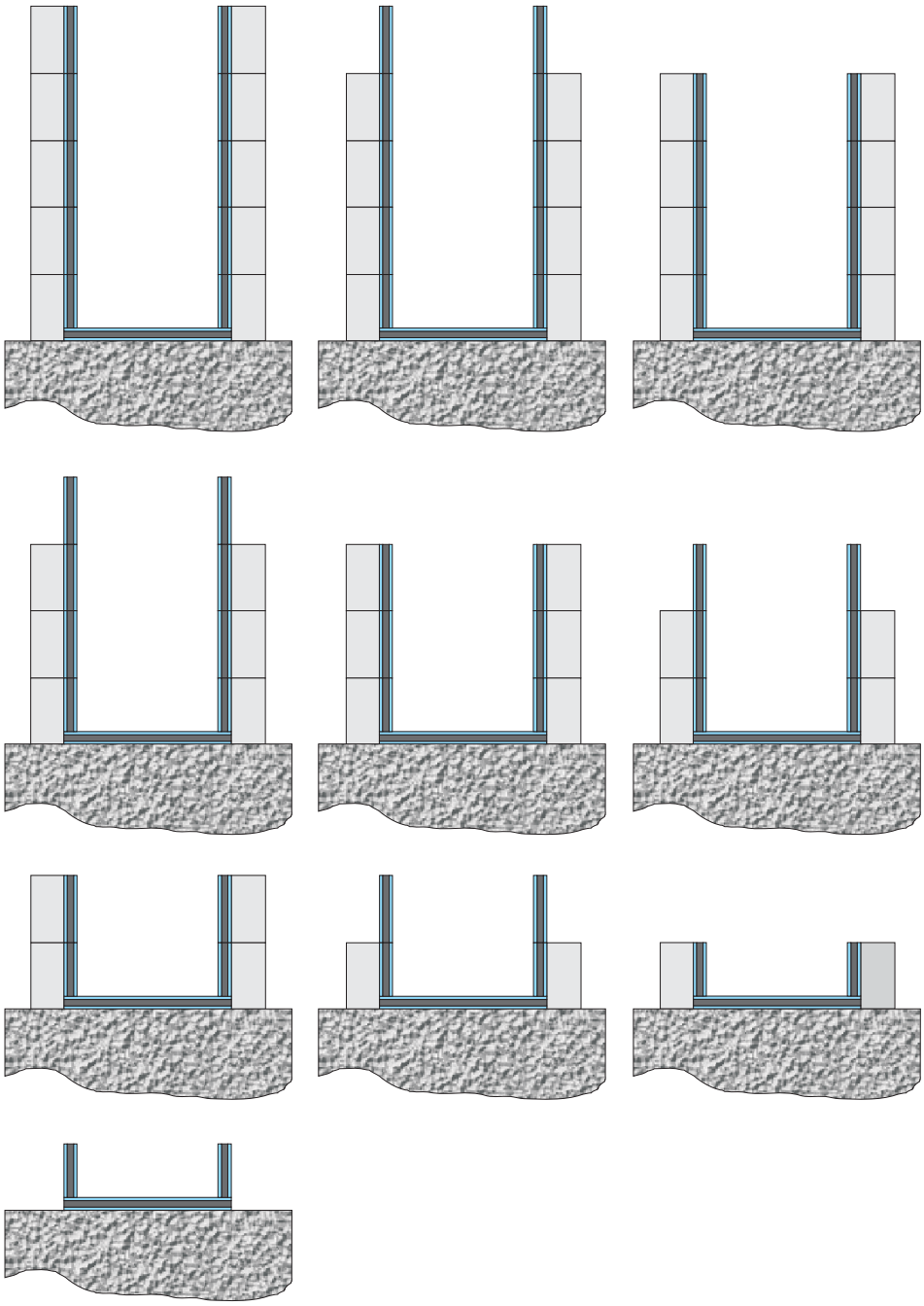

Figure 35. Dismantling the steel tanks sideways after removal of the reactor tank and the graphite reflector.

The dismantling approach is shown in Fig. 35 with 30 cm of the concrete left as shielding during the dismantling process. The dose rates at the surface of the concrete are around 1 μSv/h. Without the concrete, the dose rates at the outer surface of the tanks are around 100 μSv/h.

The reason for the moderate dose rates is the lead shield between the inner and outer steel tank. Along the centerline of the tanks the dose rate varies from around 1,000 μSv/h at the bottom of the inner steel tank to around 100 μSv/h at the top of the inner steel tank as shown in Fig. 31 at page 31.

10 Removal of reactor tank, graphite and inner steel tank

Dismantling the inner construction parts, *i.e.* the aluminium tank, the graphite reflector and the inner steel tank, might be carried out by cutting these components horizontally. In Fig. 36 the components are split into nine horizontal sections (incl. the steel bottom plate), each of which are removed sequentially from the top level. All dimensions of the sections in cm can be found in Fig. 1 at page 3.

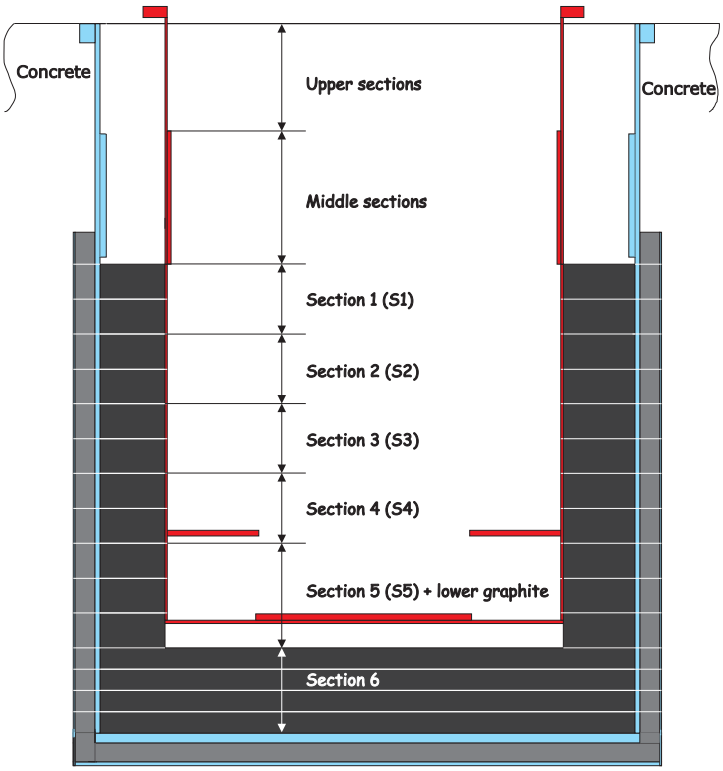

Figure 36. Vertical cross section of the DR 3 model without top shield ring.

The radiation levels one meter above the top level of the reactor with an empty reactor tank is 1 - 2 mSv/h within the diameter of the tank as shown in Fig. 16 at page 17. If the reactor tank is filled with sand, the radiation levels at the top level can be reduced by almost an order of magnitude due to shielding by the sand.

The dose rate during the horizontal cutting has been calculated for 12 situations summarised in the table below and shown in Figs. 37 and 38.

NO SECTIONS REMOVED		
(1) No sand	(2) Sand up to upper sections	
SECTIONS AND SAND REMOVED		
(3) Upper sections	(4) Sand i middle section	(5) Middle section + sand
(6) Section 1 + sand	(7) Section 2 + sand	(8) Section 3 + sand
(9) Section 4 + sand	(10) Section 5 + graphite	(11) Section 6
(12) Thick steel plate		

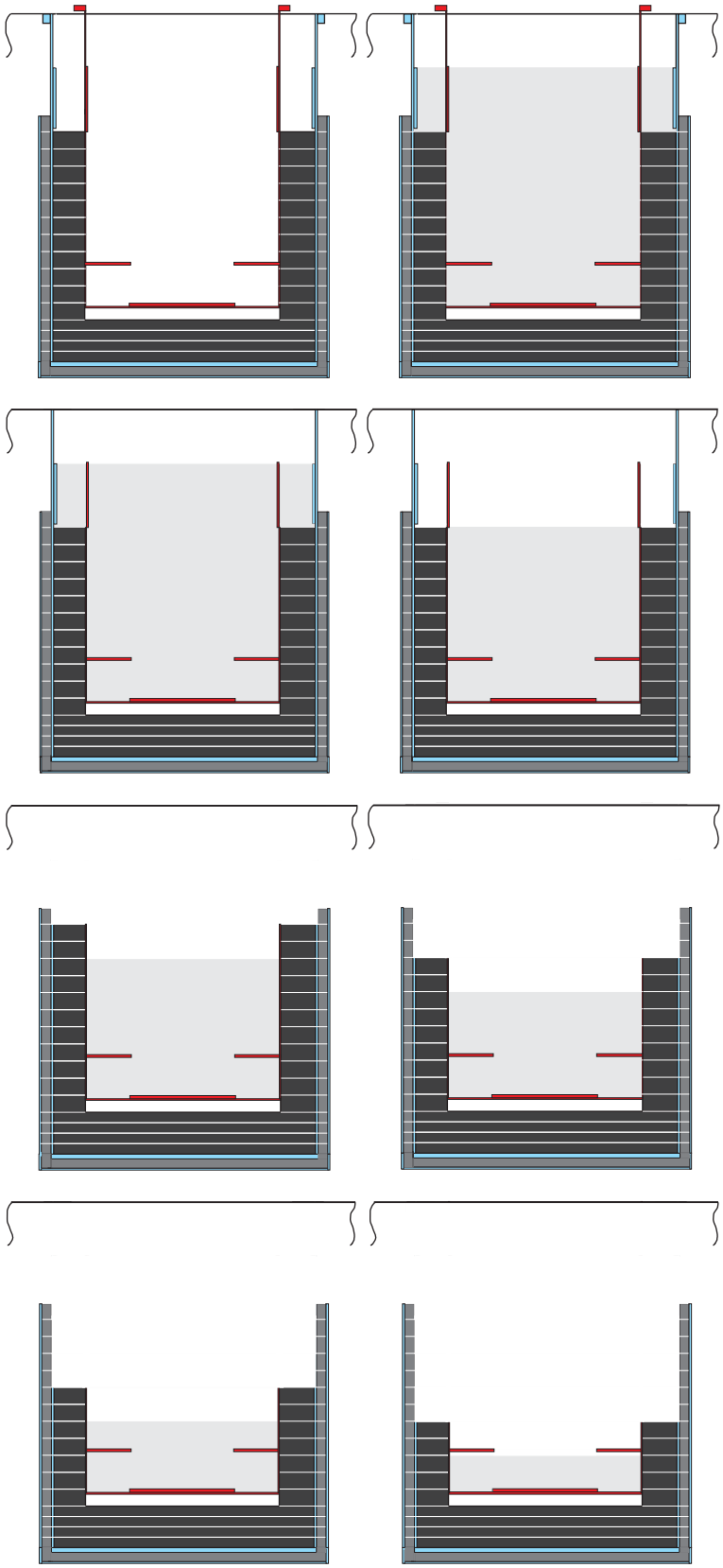

Figure 37. Illustration of horizontal cutting of reactor tank, graphite reflector and inner steel tank. The radiation levels have been calculated for each of the situations shown in Fig. 37 and in Fig. 38.

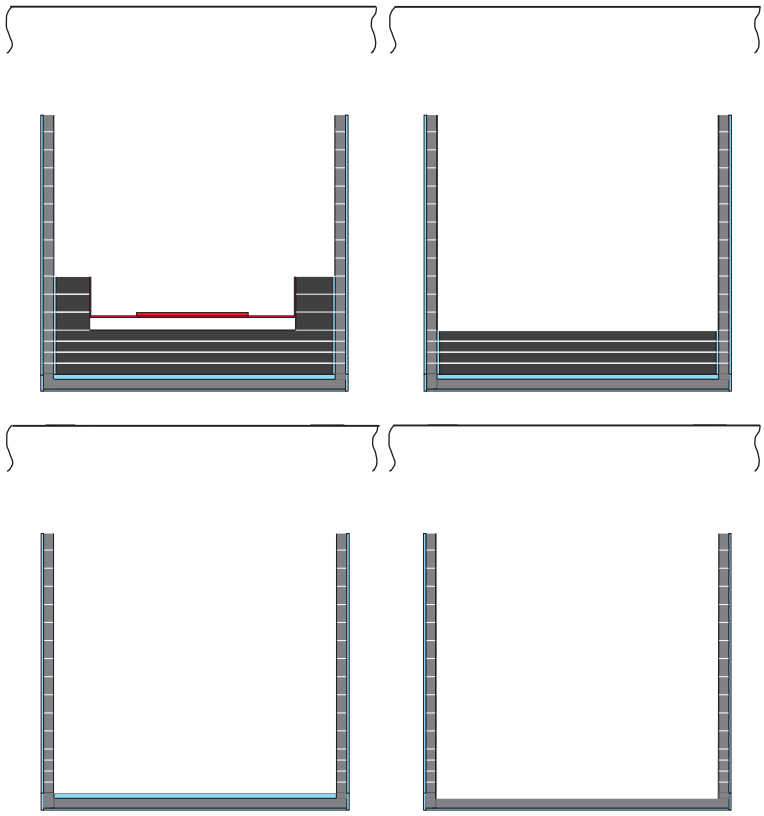

Figure 38. Illustration of the horizontal cutting - Continued.

Calculated dose rates at the reactor top for the 12 situations are shown in Fig. 39 as a function of horizontal distance from the reactor centerline.

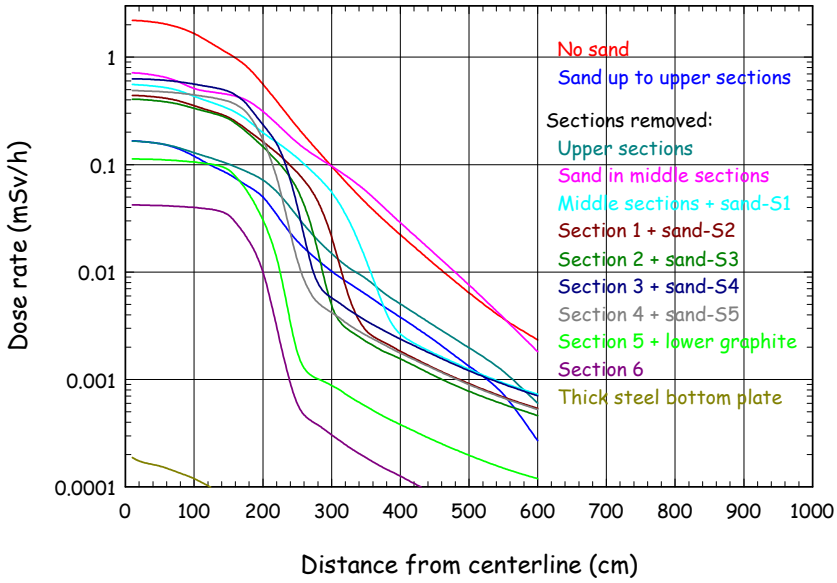

Figure 39. Dose rate from reactor tank, graphite reflector and steel tanks as a function of horizontal distance from centerline. The components are removed in horizontal sections, and the reactor tank is filled with sand up to the bottom of the section being removed. The detector points are placed 1 meter above the top floor, i.e. 411 cm above the aluminium tank bottom level.

Selected values from the graphs in Fig. 39 are shown in Table 20.

Table 20. Dose rate in μSv/h from reactor tank, graphite reflector and steel tanks as a function of horizontal distance from centerline. The components are removed in horizontal sections, and the reactor tank is filled with sand up to the bottom of the section being removed. The detector points are placed 1 meter above the top floor, i.e. 411 cm above the aluminium tank bottom level.

Sections	Horizontal distance [cm]						
	10	100	200	300	400	500	600
No sand	2,200	1,700	560	100	22	6.4	2.3
Sand to upper sections	170	120	50	10	3.8	1.3	0.3
Sections removed							
Upper sections	165	130	70	15	5.0	2.0	0.6
Sand in middle section	710	510	310	100	30	7.6	1.8
Middle section + sand	560	430	200	56	2.7	1.2	0.7
Section 1 + sand	440	350	160	20	1.8	0.9	0.5
Section 2 + sand	400	330	150	5.0	1.6	0.8	0.5
Section 3 + sand	630	560	240	5.8	2.4	1.2	0.7
Section 4 + sand	490	450	170	4.2	1.8	0.9	0.5
Section 5 + graphite	110	105	30	0.9	0.4	0.2	0.1
Section 6	42	40	10	0.3	0.1	0.06	0.04
Thick steel plate	0.2	0.1	0.05	0.02	0.007	0.0004	0.0002

Calculated dose rates one meter above the sand surface for the 12 situations are shown in Fig. 40 as a function of horizontal distance from the reactor centerline.

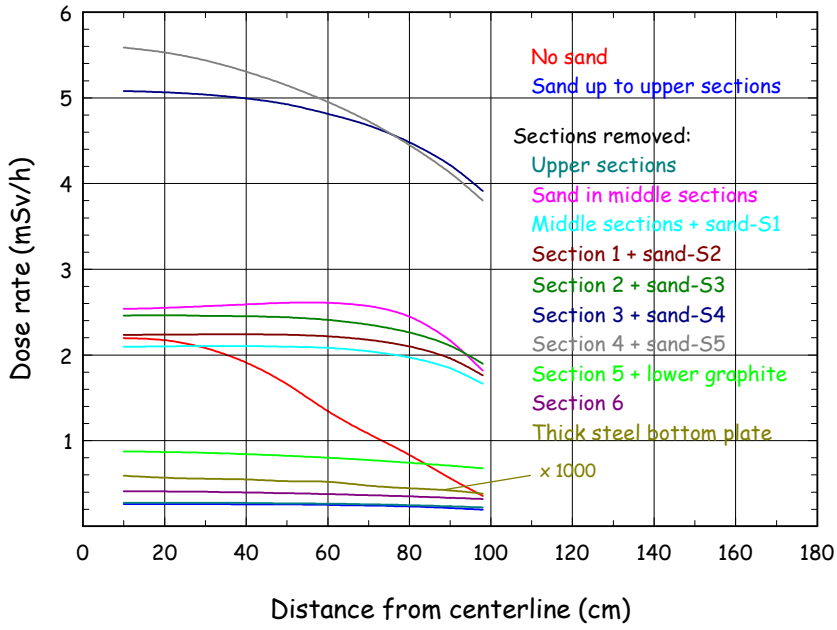

Figure 40. Dose rate from reactor tank, graphite reflector and steel tanks as a function of horizontal distance from centerline. The components are removed in horizontal sections, and the reactor tank is filled with sand up to the bottom of the section being removed. The detector points are placed 1 meter above the sand surface.

Selected values from the graphs in Fig. 40 are shown in Table 21.

Table 21. Dose rates in μSv/h from reactor tank, graphite reflector and steel tanks as a function of horizontal distance from centerline. The components are removed in horizontal sections, and the reactor tank is filled with sand up to the bottom of the section being removed. The detector points are placed 1 meter above the sand surface.

Sections	Horizontal distance [cm]								
	10	20	30	40	50	60	70	80	90
No sand	2,200	2,170	2,100	1,900	1,700	1,300	1,100	830	560
Sand to upper sections	260	260	260	258	256	250	240	230	210
Sections removed									
Upper sections	270	270	270	270	268	264	257	248	234
Sand in middle section	2,530	2,550	2,570	2,590	2,610	2,610	2,570	2,450	2,170
Middle section + sand	2,100	2,100	2,100	2,100	2,100	2,080	2,040	1,970	1,840
Section 1 + sand	2,240	2,240	2,240	2,240	2,240	2,220	2,180	2,100	1,960
Section 2 + sand	2,460	2,460	2,460	2,450	2,440	2,410	2,350	2,260	2,110
Section 3 + sand	5,100	5,100	5,040	5,000	4,930	4,810	4,700	4,500	4,200
Section 4 + sand	5,600	5,530	5,440	5,300	5,150	4,950	4,730	4,450	4,120
Section 5 + graphite	870	870	860	840	820	800	770	740	710
Section 6	410	410	400	395	390	380	360	350	330
Thick steel plate	0.6	0.6	0.6	0.6	0.5	0.5	0.5	0.5	0.4

From Fig. 39 and Fig. 40 it appears that the dose rates at the reactor top level at working distances during the horizontal dismantling of reactor tank, graphite and inner steel tank are of the order of 30 - 600 μSv/h until the bottom graphite discs have been removed. The corresponding dose rates one meter above the sand surfaces are of the order of 200 - 5,000 μSv/h.

11 Summary

The inner construction parts of the reactor DR 3 - top shield ring, reactor tank, graphite reflector, inner steel tank and outer steel tank - contains about 1 TBq of ^{60}Co at the beginning of 2012, see Table 1 at page 2. Therefore, dismantling of these components requires carefully planning with due attention to the rather high radiation levels from the various components.

The present report contains the results of Monte Carlo calculations of the radiation fields from the construction components before, during and after they have been dismantled. In all the calculations it has been assumed that the top shield plug has already been removed and safely stored outside the reactor hall.

The relative uncertainty on the calculated dose rates in this report is estimated to be 50 - 200%. This is due to the uncertainties on the activity contents in the reactor components, which are used as input to the dose rate calculations.

Section 3 contains calculated radiation fields for the following situations:

- inside and above an empty reactor tank
- inside and above a water-filled reactor tank
- above an empty and water-filled reactor tank with different steel ring shields to shield the activity in the top shield ring

- above an empty reactor tank with the best steel ring shield
- above a water-filled reactor tank with the best steel ring shield

At working positions at the reactor top (411 cm above tank bottom and 100 - 200 cm from the tank centerline) the dose rates are 3,000 - 8,000 μSv/h for an empty tank, 1,000 - 4,000 μSv/h for a water-filled tank, 600 - 3,000 μSv/h for an empty tank with a steel ring shield, and 300 - 1,500 μSv/h for a water-filled tank with a steel ring shield.

Section 4 contains calculated radiation fields from the reactor tank that has been removed in one piece to be cut in smaller parts outside the reactor hall. The top shield ring is still in place during the removal of the reactor tank. The radiation levels from the reactor tank at a few metres distance are of the order of 1,000 - 2,000 μSv/h, which allows transport of an unshielded tank to a concrete shield for a later cutting into smaller sections. The results of the Monte Carlo calculations have been compared with equivalent results of point kernel calculations and good agreement was found.

Section 5 contains calculated radiation fields after the reactor tank has been removed. The top shield ring is still in place, and radiation fields have been calculated for the following situations:

- above the reactor top level
- inside the graphite reflector

At working positions at the reactor top the dose rates are 5,000 - 13,000 μSv/h.

Section 6 contains calculated radiation fields after the top shield ring has been removed and safely stored outside the reactor hall. The reactor tank is still in place and is removed in sections, either as empty, as water-filled or as sand-filled. The sections being removed are (1) the upper section, (2) the middle (thick) section, (3) the horisontal tubes and (4) the lower sections (cylinder section and bottom/grid plate). The radiation fields have been calculated for the following situations:

- inside and above an empty tank after removal of the sections (1) - (4)
- inside and above a water-filled tank after removal of the sections (1) - (4)
- above a sand-filled tank after removal of the sections (1) - (4)

At working positions at the reactor top the dose rates for an empty reactor tank are as follows:

(1) 700 - 1,700 μSv/h after the upper section has been removed

(2) 500 - 1,400 μSv/h after the middle section has been removed

(3) 500 - 1,100 μSv/h after the horisontal tubes have been removed

(4) 100 - 300 μSv/h after the lower sections have been removed

At working positions at the reactor top the dose rates for a water-filled reactor tank are as follows:

(1) 100 - 400 μSv/h after the upper section has been removed

(2) 100 - 400 μSv/h after the middle section has been removed

(3) 400 - 1,000 μSv/h after the horisontal tubes have been removed

(4) 100 - 300 μSv/h after the lower sections have been removed

At working positions at the reactor top the dose rates for a sand-filled reactor tank are as follows:

(1) 100 - 300 μSv/h after the upper section has been removed

(2) 100 - 300 μSv/h after the middle section has been removed

(3) 400 - 900 μSv/h after the horisontal tubes have been removed

(4) 100 - 300 μSv/h after the lower sections have been removed

The reason why the dose rates increase after the horisontal tubes have been removed in the case of a water- and sand-filled reactor tank is that the water and sand levels are reduced gradually. The shielding of the bottom/grid plate is thereby reduced, and, consequently, the dose rate will increase.

Section 7 contains calculated radiation fields after the top shield ring and the reactor tank has been removed. The radiation fields have been calculated for the following situations:

- inside and above the graphite reflector and steel tanks
- along the steel tanks and graphite reflector with a 30 cm concrete shield around the tanks and graphite
- along the steel tanks and graphite reflector without a concrete shield around the tanks and graphite

At working positions at the reactor top the dose rates are 100 - 300 μSv/h.

At the side of the steel tanks, with a 30 cm concrete shield around the steel tanks, the dose rates up to 375 cm above the bottom level of the outer steel tank are 1 - 2 μSv/h for horizontal distances from the concrete surface ranging from 0 to 200 cm.

At the side of unshielded steel tanks, the dose rates up to 375 cm above the bottom level of the outer steel tank are 20 - 200 μSv/h for horizontal distances from the outer steel tank surface ranging from 0 to 200 cm.

Section 8 contains calculated radiation fields at the reactor top after different sections of the graphite reflector have been removed. The graphite sections being removed are radial layer 1 - 6 (from top), radial layer 7 - 11, bottom layer 1 - 2 and bottom layer 3 - 4.

At working positions at the reactor top the dose rates after the different graphite sections have been removed are as follows:

70 - 200 μSv/h after radial layer 1 - 6 is removed

50 - 180 μSv/h after radial layer 7 - 11 is removed

50 - 170 μSv/h after bottom layer 1 - 2 is removed

40 - 120 μSv/h after bottom layer 3 - 4 is removed

The rather modest reduction of the dose rates at the reactor top during removal of the graphite sections is because the contribution to dose rate from the removed graphite is counterbalanced by the reduced shielding of the inner steel tank by the graphite.

Section 9 contains calculated radiation fields after different sections of the inner steel tank have been removed. The sections being removed are:

(1) upper and middle (thick) section

(2) lower cylindrical section

(3) bottom plate

At working positions at the reactor top the dose rates after the different inner steel tank sections have been removed are as follows:

(1) 50 - 120 μSv/h after the upper and middle sections are removed

(2) 10 - 40 μSv/h after the lower cylindrical section is removed

(3) 0.05 - 0.1 μSv/h after the bottom plate is removed

At the side of the steel tanks, with a 30 cm concrete shield around the steel tanks, the dose rates up to 375 cm above the bottom level of the outer steel tank are 0.2 - 2 μSv/h for horizontal distances from the concrete surface ranging from 0 to 200 cm.

At the side of unshielded steel tanks, the dose rates up to 375 cm above the bottom level of the outer steel tank are 20 - 200 μSv/h for horizontal distances from the outer steel tank surface ranging from 0 to 200 cm.

Section 10 contains calculated radiation fields after horisontal sections of the reactor tank, graphite reflector and inner steel tank have been removed simultaneously. The reactor tank is filled with sand during the horizontal dismantling, and the sand is removed gradually in the dismantling process.

Nine horizontal sections have been used in the calculations: upper sections of the reactor tank and inner steel tank, middle sections of the reactor tank and inner steel tank, five sections of the reactor tank, graphite reflector and inner steel tank, one section of bottom graphite and inner steel tank and bottom plate of the inner steel tank.

At working positions at the reactor top the dose rates during the horizontal dismantling are of the order of 30 - 600 μSv/h until the bottom graphite discs have been removed. The dose rates one meter above the sand surfaces are of the order of 200 - 5,000 μSv/h.

References

[1] Ølgaard, P.L., *The DR 3 Characterization Project.* DD-23(EN), Danish Decommissioning, August 2006.

[2] Ølgaard, P.L., *Simplified DR 3 tank geometry for radiation measurements.* Internal report, Danish Decommissioning, 28 September 2008 (In Danish).

[3] Ølgaard, P.L., *Radiation sources in the top shield ring.* Internal report, Danish Decommissioning, 11 May 2009 (In Danish).

[4] Ølgaard, P.L., *Steel samples from the bottom of the top shield ring.* Internal report, Danish Decommissioning, 1 October 2009.

[5] Ølgaard, P.L., *The ^{60}Co in the TSR.* Internal report, Danish Decommissioning, 16 November 2009 (In Danish).

[6] Ølgaard, P.L., *The ^{60}Co in the TSR.* Personal communication.

[7] Søgaard-Hansen, J., *Calculation of radiation levels within and above the DR 3 reactor tank (no water in the tank).* Section of Radiation and Nuclear Safety, 26 January 2009.

DANSK DEKOMMISSIONERING

Mission

Danish Decommissioning will dismantle the nuclear facilities at the Risø-site and release buildings and areas to “green field” (unrestricted use) within a time frame of 11-20 years.

Vision

Danish Decommissioning will dismantle the nuclear facilities at the Risø-site at a high safety level so that employees, public and the environment are protected.

The decommissioning will be carried out in an economically effective manner within the budget and in accordance with international recommendations.

The decommissioning will be carried out in an open dialogue with the local population as well as with the society in general.

ISBN 978-87-7666-034-5
ISBN 978-87-7666-035-2 (Internet)

Danish Decommissioning
Post Box 320
4000 Roskilde
Telephone + 45 4677 4300
dd@dekom.dk
Fax + 45 4677 4302
Website www.dekom.dk